MEASUREMENT OF CEREBRAL BLOOD FLOW USING ARTERIAL SPIN LABELING METHOD ACROSS LIFESPAN

by

CIWEN WANG

Presented to the Faculty of the Graduate School of

The University of Texas at Arlington in Partial Fulfillment

of the Requirements

for the Degree of

MASTER OF SCIENCE IN BIOMEDICAL ENGINEERING

THE UNIVERSITY OF TEXAS AT ARLINGTON

August 2015

Copyright © by Ciwen Wang 2015

All Rights Reserved

Acknowledgements

I would like to express my gratitude to Dr. Hanli Liu, Dr. Takashi Tarumi and Dr. Rong Zhang for offering me a chance to work on MRI data processing. They are all very supportive and understanding. I am very grateful for all the opportunities and knowledge I gain in Dr. Liu's courses. Her teaching lays a very good foundation for my MRI knowledge. I am very grateful for Dr. Tarumi's patient and inspiring teachings. I am extremely inspired by his work. I am very grateful for Dr. Zhang's instructions, especially in physiology.

I am extremely thankful to Dr. Liu, Dr. Zhang and Dr. Mingwu Jin for being on my thesis defense committee, although they are all very busy, they all give me valuable advises.

I am very thankful to Dr. Hanzhang Lu and Dr. Peiying L. Wang for their instruction in ASL sequence and ASL data processing. I am thankful for their ASL processing Matlab code and instructions.

I want to thank all my friends who encourage me and cheer me up. Finally, I want to thank my father Mr. Zhongde Wang for supporting and encouraging me throughout my life.

July 29, 2015

Abstract

MEASUREMENT OF CEREBRAL BLOOD FLOW USING ARTERIAL SPIN LABELING METHOD ACROSS LIFESPAN

Ciwen Wang, M.S.

The University of Texas at Arlington, 2015

Supervising Professor: Hanli Liu

Arterial Spin Labeling (ASL) is one family of perfusion-weighted contrast imaging techniques of Magnetic Resonance Imaging (MRI) that measures cerebral blood flow by labeling spins in arterial blood with inversion and then waiting for a certain period of time for the labeled arterial blood to enter the imaging plane, and then acquiring MR image at the image plane. In compare with PET, ASL is a noninvasive new technology. But as a new technology, it is not very commonly used because of the relatively low signal to noise ratio, less robust mechanism, and more important, there is no standard for clinical applications. One goal of this study is to find out the optimal imaging processing way and parameters for ASL processing. The other goal is to find the relationship between CBF and age. There are 173 subjects, with 107 female subjects and 66 male subjects.

Pseudo-continuous ASL (PCASL) was used as labeling sequence and multi-slice single shot 2D Echo-planar imaging (EPI) was used as MR image acquisition sequence. 40 pairs of control – labeled images were taken in order to increase signal to noise ratio. An MPRAGE T1 image was taken for each subject as brain structure reference. Label duration = 1650ms; post label delay = 1525ms; TR = 4260ms or 4210.8ms; TE=14ms. EPI factor = 35ms. Voxel size = 3×3×5 mm; FOV = 240×240×145 mm; slice number = 29.

FSL which is a MRI image processing tool developed by Oxford was used in imaging processing. dcm2nii was used for DICOM to NIFTY conversion. MCFLIRT was used for motion correction. Trilinear interpolation was used in MCFLIRT. In spatial smoothing, a 3D Gaussian kernel with FWHM = 6mm was used.

In M0 magnetization baseline calculation, the average magnetization of the whole brain of mean control image was used, so that the T1 recovery time was assumed to be the time from labeling to image acquisition of the middle slice (15th slice). The longitudinal relaxation time of blood was used as T1 value of the tissue. In Cerebral Blood Flow (CBF) calculation, also the longitudinal relaxation time of blood was used as T1 value of the tissue.

A threshold of 0 – 300 was used on the CBF map. Voxels below 0 was assigned 0, and above 300 was assigned 300. CBF map was first co-registered on the T1 structural image of the same subject, and then, with the help of the high resolution T1, CBF map was normalized on MNI152 template.

Relative CBF map was calculated by dividing the value of each voxel by the mean value of the whole brain CBF.

The voxelwise analysis results ($p < 0.05$) on both CBF and relative CBF show that CBF decline is most significant in prefrontal cortex and the area around the ventricles during aging. CBF of occipital lobe was not affected by aging too much. It is difficult to say if CBF in white matter is not affected by age, or it is the relatively long arterial transit time of white matter that causes this problem.

The results of ROI CBF extraction also show that CBF of frontal, prefrontal, temporal cortex and hippocampus, especially right hippocampus has strong negative relationship with aging. CBF of white matter does not affected by aging.

Table of Contents

Acknowledgements iii

Abstract iv

List of Illustrations viii

List of Tables x

Chapter 1 Introduction 1

1.1 Clinical Neuroradiology 1

1.1.1 Magnetic Resonance Imaging 2

1.1.2 Perfusion imaging 5

1.1.3 Arterial Spin Labeling theory 7

1.1.4 Cerebral Blood Flow (CBF) Calculation 9

1.2 Cerebral Blood Flow 11

1.2.1 Magnetic Resonance Imaging 11

1.2.2 Cerebral Metabolism and Blood Supply 12

1.2.3 Cerebral Blood Supply and Aging 13

1.3 Focus of this Study 14

1.4 Outline of this Thesis 15

Chapter 2 Arterial Spin Labeling Image Acquisition 16

2.1 Ethical Approval and Subjects 16

2.2 MRI Sequence 17

2.2.1 Arterial Spin Labeling Image 17

2.2.2 T1 Image 18

Chapter 3 Arterial Spin Labeling Image Processing 20

3.1 Preprocess 20

3.2 ASL Perfusion Calculation 22

3.3 Cerebral Blood Flow Threshold and Registration 26
Chapter 4 Data Processing and Results 28
4.1 Data Processing and analysis 28
4.2 Results 29
Chapter 5 Discussion and Future work 66
5.1 Discussion 66
5.2 Limitations 67
5.3 Future Work 68
References 70
Biographical Information 74

List of Illustrations

Figure 2-1 Subject Age Distribution Histogram 19

Figure 4-1 Design Matrix of Voxelwise Analysis 29

Figure 4-2 The Voxelwise Analysis Result of CBF 30

Figure 4-3 The Voxelwise Analysis Result of rCBF 31

Figure 4-4 CBF of whole brain 33

Figure 4-5 CBF of Frontal lobe 34

Figure 4-6 CBF of Occipital lobe 35

Figure 4-7 CBF of Parietal lobe 36

Figure 4-8 CBF of Temporal lobe 37

Figure 4-9 CBF of Cerebral Cortex Left 38

Figure 4-10 CBF of Cerebral Cortex Right 39

Figure 4-11 CBF of White Matter Left 40

Figure 4-12 CBF of White Matter Right 41

Figure 4-13 CBF of Hippocampus Left 42

Figure 4-14 CBF of Hippocampus Right 43

Figure 4-15 CBF of Prefrontal Cortex Left 44

Figure 4-16 CBF of Prefrontal Cortex Right 45

Figure 4-17 CBF of Cingulate Cortex Posterior Left 46

Figure 4-18 CBF of Cingulate Cortex Posterior Right 47

Figure 4-19 CBF of Precuneus Cortex Left 48

Figure 4-20 CBF of Precuneus Cortex Right 49

Figure 4-21 rCBF of Frontal lobe 50

Figure 4-22 rCBF of Occipital lobe 51

Figure 4-23 rCBF of Parietal lobe 52

Figure 4-24 rCBF of Temporal lobe 53
Figure 4-25 rCBF of Cerebral Cortex Left 54
Figure 4-26 rCBF of Cerebral Cortex Right 55
Figure 4-27 rCBF of White Matter Left 56
Figure 4-28 rCBF of White Matter Right 57
Figure 4-29 rCBF of Hippocampus Left 58
Figure 4-30 rCBF of Hippocampus Right 59
Figure 4-31 rCBF of Prefrontal Cortex Left 60
Figure 4-32 rCBF of Prefrontal Cortex Right 61
Figure 4-33 rCBF of Cingulate Cortex Posterior Left 62
Figure 4-34 rCBF of Cingulate Cortex Posterior Right 63
Figure 4-35 rCBF of Precuneus Cortex Left 64
Figure 4-36 rCBF of Precuneus Cortex Right 65

List of Tables

Table 3-1 Parameters of M0 and CBF Calculation 25

Table 4-1 Voxel count of CBF negative correlated with age in 16 ROI 31

Table 4-2 Voxel count of rCBF positive/negative correlated with age in 16 ROI 31

Table 4-3 Mean Resulting CBF and rCBF in Whole Brain and 16 ROI 32

Table 4-4 The Correlation Coefficient of CBF/rCBF with Age

in Whole Brain and 16 ROI 32

Chapter 1

Introduction

1.1 Clinical Neuroradiology

Neuroradiology is one branch of radiology focusing on characterizing abnormalities of nervous system. Neuroradiology uses neuroimaging technology to image the structure, function, and perfusion of the nervous system. Computed tomography (CT) and magnetic resonance imaging (MRI) are often used in doing structural neuroimaging. Positron emission tomography (PET), functional magnetic resonance imaging (fMRI), and perfusion MRI are often used in doing functional neuroimaging.

Computed tomography (CT) uses computer to combine a lot of X-ray attenuation images taken from different angles to produce cross-sectional images, which represents the X-ray attenuation properties of specific body areas.

Positron emission tomography (PET) is one kind of nuclear medicine imaging. Radionuclide tracer is used in PET scan. Pairs of gamma rays emitted by the tracer are detected by the system, and 3D images are produced about the functional processes of the body. ^{15}O-water positron emission tomography is used to detect perfusion of the brain as a golden standard [1].

Positron emission tomography and Computed tomography are often used together to create function images upon clear anatomical structural images. A lot of modern machines are able to perform CT scan together with PET scan during the same session on the patient.

The downside of PET is that it is invasive. Exogenous contrast agent needs to be injected into the body before a PET scan. PET uses gamma rays and CT use X-rays, and

both gamma ray and X-ray are harmful to the body, because they have very high photon energy that can knock electrons in human tissue out of their nucleus.

Magnetic resonance imaging (MRI) is relatively safe, because it is free of radiation. Perfusion MRI can use either exogenous or endogenous contrast tracer. Both exogenous and endogenous contrast just freely go though the vascular system, and the attenuation of magnetic resonance signal in each location represents how much of the contrast agent is there [2].

Arterial spin labeling uses endogenous tracer, so that it is non-invasive and safe to patients.

1.1.1 Magnetic Resonance Imaging

Magnetic resonance imaging (MRI) uses strong magnetic fields to create images of tissue. It takes advantage of the physical phenomenon that is called nuclear magnetic resonance (NMR). The phenomenon of NMR was known since 1940s, and this physical phenomenon was used in imaging in 1973 by Paul C. Lauterbur [3]. NMR phenomenon is when nucleus with odd number of protons are placed in a magnetic field, they will absorb electromagnetic radiation at some certain frequencies, and re-emit the electromagnetic radiation they absorbed. Only nucleuses that have both spin angular momentum and magnetic moment in association with an external magnetic field have NMR property. These nucleuses are called spins and can be used in nuclear magnetic resonance imaging. Hydrogen nucleus is often used in MRI imaging because it has NMR property and is very abundant in human body because human bodies have high water content.

Spins initiate precession, a gyroscopic motion aligns with an axis in the presence of a strong external magnetic field. When a strong external magnetic field like 3 Tesla B0 is given, spins precess around an axis parallel or antiparallel to the B0 magnetic field. The type of nucleus and the strength of the external magnetic field determine the

frequency of spins precession. The resonant frequency of a spin in an external magnetic field with certain strength like 3 Tesla is called Larmor frequency. Spins precess around an axis parallel to B0 have lower energy than the spins precess around an axis antiparallel to B0. When electromagnetic energy is sent to the spins at Larmor frequency to meet the energy gap, spins that precess around an axis parallel to B0 get enough energy to precess around an axis antiparallel to B0. The Larmor frequency of hydrogen nuclei is 42 MHz per Tesla of static magnet field [2]. Excitation is providing radiofrequency energy to spins at Larmor frequency to change some spins from low-energy to high-energy state. When the number of spins in low-energy and high-energy state is the same, then, there is no net magnetization along the longitudinal direction. The excitation pulse that achieves this effect is called 90-degree excitation pulse. In this state, net magnetization only precesses in transverse plane. The excitation pulse that gives the spins exactly sufficient electromagnetic energy to reverse the numbers of low-energy spins and high-energy spins is called 180-degree excitation pulse. After the radiofrequency pulses are turned off, the excess spins with high-energy level release energy and go back to low-energy state. The energy they release is equal to the energy corresponding to Larmor frequency. A radiofrequency coil tuned to the Larmor frequency can be used to detect the changes in transverse magnetization right after radiofrequency pulses turn on and off. This change detected by reception coils constitutes the MR signal, and MR image is created according to this MR signal.

The spatial information of the image is encoded by the gradient fields. Gradient fields change the strength of static magnetic field by superimposing a series of linear magnetic strength gradients from minimum to maximum in x, y, z direction. X-gradient is from left to right; Y-gradient is from back to front; Z-gradient is from bottom to top. Spins under greater magnetic gradient will precess faster than spins under smaller magnetic

gradient. As long as the precession speed of spins in each location is identical, we can use it to encode the location.

Although most MRI images are 3D, they are composed of a series of x-y plane 2D images. A set of x-y plane images is stacked along z direction to create a 3D image.

The art of creating medical image is different contrasts. Without contrasts, medical images are meaningless. MRI has a lot of ways of making contrast. For example like proton density contrast, chemical concentration, relaxation time contrast, motion contrasts and so on. In this experiment, T1 relaxation time contrast and motion contrast are used. Proton-density image provides contrast based on the number of protons in a voxel, which is different for different tissue type.

T1 contrast takes advantage of the difference in the relaxation properties of nuclei. Different tissue has different number of a certain kind of nuclei, like hydrogen nuclei. The relaxation property of hydrogen nuclei is used in this experiment. The tissue that has a shorter T1 value recovers more rapidly and thus has greater MR signal. In a T1 weighted image, white matter has greater MR signal than cerebral spinal fluid or gray matter.

T2 contrast also depends on the relaxation properties of nuclei. T2 weighted image has maximal signal in fluid-filled regions.

The contrasts of MR image depend a lot on the pulse sequence. There are two very important parameters in pulse sequence: repetition time (TR) and echo time (TE). Repetition Time (TR) is the time interval between two successive excitation pulses. Echo time (TE) is the time between the start of the excitation pulse and the maximum in the signal, which is also the time of data acquisition. Proton-density contrast often uses very long TR and very short TE. A T1 image is very often used in creating anatomical images

of the brain. It uses a moderate length of TR and very short TE. In this experiment, the TE is very short, so that T2 relaxation effects are not considered.

In functional imaging and perfusion imaging, images have to be acquired very rapidly. In order to acquire a large number of images in short periods of time, special image acquisition sequence is used to acquire images fast. Echo-planar imaging (EPI) is used in data acquisition in this experiment. This sequence was invented by Mansfield in 1977 [2]. Using this sequence, the entire k-space is filled by switching gradient rapidly after a single excitation pulse. Very strong gradients are needed to perform EPI. The imperfection in the magnetic fields will cause EPI artifacts that cause signal lose especially at the boundary of brain tissue and air-filled cavities. Because the whole 2D image is acquired after a single excitation pulse, the readout time is quite long, and it will cause geometric distortion.

1.1.2 Perfusion imaging

Perfusion is very important for tissue function, because tissue needs oxygen and other nutrients from arterial system and drains the metabolic wastes into vein.

Perfusion is the irrigation of tissue through the arterial system. Perfusion is expressed as the volume of blood that travels through a tissue mass over time [2]. Perfusion of brain tissue is very important. If there is any abnormal or disruption in brain perfusion, profound effects will be caused, for example, coma and brain damage. Perfusion alteration in brain commonly accompanies some neurological problems like Alzheimer disease, other neurodegenerative diseases, brain cancer and so on. Perfusion MRI can be used to assess intracranial tumors and stroke. The physiological unit used for perfusion is mL/min/100g(blood flow rate (mL/min) / 100g tissue mass).

Perfusion MRI is used to generate images of blood flow, especially blood flow in capillaries and other small vessels. It can get different physiologic parameters like blood

volume, blood oxygenation and blood velocity. It may use either endogenous or exogenous contrast. The attenuation of the MR signal in each voxel is proportional to the amount of the contrast agent present. Thus, signal changes can be interpreted as a function of perfusion, and images can be created that depict different perfusion properties such as relative cerebral blood flow (rCBF) and so on [2]. Two techniques are commonly used to measure cerebral perfusion in MRI field. One is Arterial spin labeling (ASL) which uses an endogenous tracer. The other uses an exogenous intravascular tracer, which is usually a gadolinium-based tracer. Using gadolinium-based contrast agent, perfusion-weighted imaging which is known as Dynamic Susceptibility Contrast-Enhanced MR Perfusion (DSC MR) can be acquired through T2 or T2* MRI. With this tracer, permeability MRI, which is also known as Dynamic Contrast-Enhanced MR Perfusion (DCE MR), can be acquired through T1 MRI. DSC MR and DCE MR are considered more robust than ASL. DSC MR is widely used to detect brain tumors. DCE MR is used to examine the microvasculature of the brain in order to assess brain tumor angiogenesis. Of course using exogenous tracer has advantages over ASL. First of all, DSC and DCE have higher signal to noise ratio than ASL, so that they can generate images at higher spatial and temporal resolution. Secondly, DSC MR can generate the 3D image of the brain in less than 1 minute, while ASL has to take 3-4 minutes. A significant longer image acquisition time will cause more potential motion artifacts, because it is difficult to keep a patient motionless in a long period of time. ASL is very sensitive to motion, because it uses subtractive technique. Finally, severe ischemic patients who have longer arterial transition time might cause the labeled signal decays more and an underestimation of CBF [4].

1.1.3 Arterial Spin Labeling theory

Arterial spin labeling (ASL) is a family of perfusion imaging techniques that measure blood flow by labeling spin with inversion pulses and then waiting for the labeled spins to enter the imaging plane before data acquisition. The labeled images contain signals from both labeled water, which flows from the label plane, and the static tissue water at the image plane. Control images without arterial spin labeling are acquired separately. The subtraction of control and labeled image is the signal from labeled water. It uses endogenous contrast that is water proton in arterial blood, so that it is noninvasive. ASL labels the magnetization by inversion. There are two kinds of ASL: continuous ASL and pulsed ASL. In pulsed ASL, a bolus of arterial blood is labeled and passes through the tissue as a transient; in continuous ASL, the labeled arterial blood establishes a steady time [5]. Continuous ASL uses longer labeling bolus than pulsed ASL, and have higher signal to noise ratio. Because labeling slab does not compete with imaging slice, continuous ASL has better spatial coverage. But continuous ASL is more demanding on hardware and generates more heat. There are continuous ASL and pseudo-continuous ASL. Pseudo-continuous ASL applies larger gradients during RF pulses and thereby increases the resonant offset of the pulses relative to brain tissue, and thereby decreasing magnetization transfer effects which can cause signal loss substantially larger than the perfusion-induced signal change [6]. Pulsed ASL has a higher labeling efficiency and less RF power deposition.

The basic principle of arterial spin labeling is using the magnetization of water protons in the arterial blood stream as an endogenous contrast. Any perturbation to the magnetization of the arterial blood that feeds the tissue can serve as a magnetic contrast. Although continuous ASL, pseudo-continuous ASL and pulsed ASL are all available, pseudo-continuous ASL is recommended because of the reasons mentioned above. In

this experiment, pseudo-continuous ASL is used, so that only pseudo-continuous ASL is discussed here. In pseudo-continuous ASL (PCASL), more than one thousand shaped RF pulses are applied at a very high rate. The spacing from the center of one pulse to the center of the next pulse is about 1 ms [6]. This PCASL inversion pulse is used at an upstream location proximal to the tissue of interest. Then, wait for a certain time period to let the labeled arterial blood to reach the capillary bed of the tissue of the imaging plane. The exchange of water molecules and magnetization between the labeled water and the water in the tissue of the image plane causes a change in MR signal. Then, an imaging sequence is played to acquire an image at the imaging plane. Subtracting this labeled image from a control image without RF inversion pulse creates the spatially resolved signal change image. Perfusion quantification relies on the signal change between the control image and the labeled image, and this signal change is only 1-2% [5]. So, it is very important to get rid of other factors that can cause signal variation. In the MRI signal acquisition aspect, a 180-degree inversion pulse might be helpful for background suppression, especially in the segmented 3D readout GRASE sequence.

We have too many choices in ASL to make the ASL being accepted in clinical community, so that a standard is needed to make ASL results comparable between different sites, and establish meaningful clinical trials. In image acquisition, different TE, TR, label duration and post label delay can be used which will of course cause different results. Mean transit time (MTT) is the average time for the tracer to pass through the tissue [7]. Post label delay depends a lot on it, but the MTT of labeled spins in the water of the arterial blood is quite long. It is difficult to decide which post label delay is the best, because a short post label delay does not allow enough time for the labeled blood water to completely deliver to the tissue, but a long post label delay results in strong T1 decay, and a low signal to noise ratio. Post label delay time has to be shortened in order to

guarantee the signal strength. So, low ASL signal might be caused by low CBF or long arterial transit time (ATT). If ATT is needed to be estimated, a multiple post label delay should be used. As long as a single post label delay is used in this experiment, multiple post label delay will not be discussed. Longer label duration increases ASL signal and signal to noise ratio, but this also increases the TR duration, and decreases the number of image slices obtained per unit of time. There are several methods of choosing the location of labeling plane. The labeling plane should be somewhere that contains arteries relatively straight and perpendicular to the labeling plane. But it is difficult to find a plane like this. Angiogram is helpful to find a good labeling plane if available. In many cases, the labeling plane is right below the cerebellum. A labeling plane that is 84 mm below the anterior commissure-posterior commissure line yields the highest sensitivity [8].

Multi-slice single shot 2D EPI is often used in ASL image readout, although segmented 3D sequence is considered the best option [6]. Single shot EPI is available on all MRI systems and is less sensitive to the artifacts caused by a motion within one scan.

Of course other techniques like parallel imaging using multichannel coils and vascular crushing gradients (spoiling gradient) to reduce vascular artifacts can also be used in ASL.

1.1.4 Cerebral Blood Flow (CBF) Calculation

The basic theory of getting CBF in ASL is doing control image minus label image. But calibration is needed to make the (control – label) meaningful in scientific aspect. So, a CBF calculation is needed after getting the control and label images.

With only T1 decay, MR signal in each imaging voxel is: $M(t) = M0 + C \cdot e^{-t/T1}$. C is unknown and determined by the initial magnetization M(0), which is Z magnetization at time 0 after RF excitation. As long as M(0) is assumed to be 0, C=-M0. So that MR signal in each imaging voxel: $M(t) = M0 \cdot (1 - e^{-\frac{t}{T1}})$. M0 is the original magnetization,

which is the net magnetization (the difference between the number of spins in parallel to B0 state and number of spins in antiparallel state) in the x-y plane before relaxation. So, M0 is the baseline of Z magnetization. It needs to be known in advance. Of course, the M0 in each voxel is different, so that signal intensity of a proton density weighted image can be used as baseline instead of M0. But while it is not available, the average M0 of the whole 3D control image is used as baseline. ASL sequence has a quite long TR and a very short TE, so that control image without labeled sequence is almost like a proton density weighted image. Labeled image cannot be used to calculate M0, because the inverse pulse flipped the signal from M0 to –M0.

So, M0 is calculated through the longitudinal magnetization of control image.

Longitudinal magnetization of the tissue: $M_{tissue} = M0 \cdot \left(1 - e^{-t/T1_{tissue}}\right)$

So that $M0 = \frac{M_{tissue}}{\left(1-e^{-t/T1_{tissue}}\right)}$

Cerebral blood flow calculation is based on a formula compartment model of water diffusion from the Bloch equation for brain water magnetization [2]:

$$\frac{dM_z(t)}{dt} = \frac{M0 - M_z(t)}{T_1} + f\left(M_{arterial}(t) - M_{venous}(t)\right)$$

In this formula, $\frac{dM_z(t)}{dt} = \frac{M0-M_z(t)}{T_1}$ is just the longitudinal magnetization part of Bloch equation, because labeled blood only changes the longitudinal magnetization. $f\left(M_{arterial}(t) - M_{venous}(t)\right)$ is the CBF part. f is the blood flow in mL/g/sec. $M_{arterial}$ is the Z magnetization per ml of arterial blood. M_{venous} is the magnetization per ml of venous blood. Because M_{venous} is unknown, It is assumed that $fM_{venous} = fM_{brain}/\lambda$. Mbrain is the A magnetization per gram of brain tissue, and λ is brain-blood partition coefficient, which was defined as (quantity of water/g of brain)/(quantity of water/ml of blood) [23].

This formula is based on the assumption that water instantaneously equilibrates throughout the voxel, so that the magnetization of the blood leaving the voxel is the same as the rest of the voxel.

1.2 Cerebral Blood Flow

1.2.1 Cognitive Function Decline and Aging

We all know that neural system changes throughout our lives. When infants are born, they have much more neurons than adults. Neural axons compete with each other. Only neurons that make synapse with appropriate postsynaptic cells, which provide neurons with nerve-growth factor, can survive. This neural Darwinism is the way for us to get the right number of neurons in each area of the nervous system. Which neurons can survive depends a lot on experience. Neural dendrites and axons also continue to change their structure throughout our lives. It is also experiences that guide the neurons to change. So, the neural systems of different people are quite different. The conclusions of studies on neural system can only be based on statistical analysis. We can only say that on average the memory and reasoning function of human fade beyond age ~ 60 years old. Brain shrinks with age because of neuron-degeneration, but the degeneration varies a lot among different people. From age 20 to 90, the brain loses 5-10 percent of its weight on average because of the decrease in dendrites and damage of the myelin sheath [9]. The thickness of the temporal cortex shrinks by about half a percent per year on average [10]. The frontal cortex begins to shrink at age 30 [11]. The degeneration of neural system causes general slowing of function in central nervous system, which in turn affect both intellectual performance and physical coordination. Some areas degenerate more than other areas. The prefrontal cortex and hippocampus are the areas shrinking more than other areas when people are old. The production of neurotransmitters also

reduces in aging people. Some researchers found that declines in memory function might be associated with the reduction of acetylcholine production, and carrying out motor activities and planning problems might be related to the normal age related reduction of dopamine production [9]. But it does not mean that every older adult would experience a significant cognitive function decline, because average is just average. People vary a lot. Besides, brain has remarkable compensation and repairing capability. Older people may use more brain areas to compensate, and they have greater world knowledge and experience. So the influences of age on different older people vary a lot.

1.2.2 Cerebral Metabolism and Blood Supply

Cerebral Blood Flow (CBF) is how much blood irrigates the brain during a certain period of time. It is regulated by the metabolic demands of brain tissue. The higher the cerebral metabolic rate, the more arterial blood carrying oxygen is needed. So, cerebral blood flow is quite representative of the daily function of the brain. Regional hypo-perfusion might be related with accumulation of amyloid and cognitive deficits [12].

Of course, other parameters like cerebral metabolic rate of oxygen (CMRO2), and venous blood oxygenation are also good indicators of cerebral metabolism. The brain consumes about 20% of the total energy in human body [13]. Arterial blood carries oxygen to the brain, and the oxygenated blood flows into capillary beds, a certain percentage of oxygen is exchanged by brain tissue with carbon dioxide, finally, the blood with lower oxygen concentration is drained through veins.

Magnetic resonance imaging (MRI) experiment on Cerebral Blood Flow (CBF), cerebral metabolic rate of oxygen (CMRO2), and venous blood oxygenation can be used together to assess neurovascular diseases that affect the cerebral metabolism. The reduction of CBF might be caused by decreased oxygen demand or vascular problem. The ability of vessels to dilate affects the cerebral blood flow. An increasing of cerebral

metabolic rate of oxygen (CMRO2) and decreasing of cerebral blood flow might indicate a vessel problem. Positron emission tomography (PET) experiment on metabolic rate of oxygen (CMRO2), cerebral blood flow (CBF) and oxygen extraction fraction (OEF) can also be used to determine cerebral energy metabolism and blood flow.

1.2.3 Cerebral Blood Supply and Aging

CBF is important to indicate healthy aging of the brain. When a person gets old, he or she is vulnerable to vascular disease as well as neural problem. Arteriosclerosis is quite common in elder people. The walls of the arteries become thicker, harder, and lose elasticity. Arteries are no longer elastic enough to dynamically adjust cerebral blood flow. Many older people also get atherosclerosis. Their arterial walls not only become thicker, harder and less elastic, but also have fatty streaks. This pathological change of arterial walls makes the diameter of the arterial lumen even smaller. Of course both arteriosclerosis and atherosclerosis decrease cerebral blood flow, because it is more difficult for the heart to pump the blood into the brain, and it is also more difficult for the arterials to dilate to meet the needs of the brain. The power of heart to squeeze and pump blood out also seems to decline when people get old. On the other hand, the degeneration on neurons in older people might also cause the decreases of cerebral blood flow.

It is important to know the cerebral blood flow changes in normal aging, so that we can compare these changes with pathological cerebral blood flow changes in Alzheimer's disease, mild cognitive impairment, ischemic stroke and so on.

One study, which used MRI to measure Cerebral Blood Flow (CBF), cerebral metabolic rate of oxygen (CMRO2), and venous blood oxygenation, indicates that aging causes CMRO2 to increase significantly, and CBF to decrease [14]. This result means

that the blood supply to the brain diminishes while the oxygen demand of the brain is still quite high.

Another study, which used PET to measure metabolic rate of oxygen (CMRO2), cerebral blood flow (CBF) and oxygen extraction fraction (OEF), indicates that aging causes CBF and CMRO2 to decrease in large parts of the cerebral cortex, but no significant decrease in motor and sensory cortex or occipital cortex [15]. So that age related change in CBF and CMRO2 are different in different brain areas.

1.3 Focus of this Study

Magnetic resonance imaging (MRI) is a technique, which takes advantage of the magnetic property of spins to create images of tissue. MRI is commonly used in medical field. Arterial spin label (ASL) is a technique, which uses MRI technology to get the information of cerebral blood flow (CBF). Although positron emission tomography (PET) is still the golden standard of measuring CBF and CMRO2, MRI technology becomes more and more mature in measuring these parameters. But as mentioned before, because of lacking a standard of measuring CBF, ASL is not as commonly used as PET, although ASL has a lot of advantages over PET.

The aim of this study is to use ASL technology to measure CBF of people with different ages, and find out the best parameter values in CBF calculation. Of course, the relationship between CBF and age is also one aim of this study. As mentioned before, in calculating CBF, there are a lot of assumptions. How to pick up an optimal value for each parameter is quite important. Besides, other image processing technologies like motion correction, smoothing also affect the result of CBF calculation.

Because all CBF maps are registered into MNI152 standard template, CFB of each region extracted and compared according to age using masks created from MNI152 atlas. Not too many studies did regional cerebral blood flow extraction on CBF maps

created by ASL technology. PET is the golden standard of doing things like this. According to the PET study mentioned above, age-related CBF changes in different brain regions are different. Collecting data about age related CBF change in different brain regions from ASL flow map makes it possible to compare CBF data of ASL with PET. The comparing result is useful to study ASL in the future.

1.4 Outline of this Thesis

Chapter 1 discussed the theory and technology of magnetic resonance imaging (MRI), the theory and technology of measuring cerebral blood flow, and the relationship between age and cerebral blood flow. Chapter 2 describes the process of ASL image acquisition from a Philip MRI machine and the theory behind it. Chapter 3 describes the image processing part of ASL, from image file format conversion to the registration of ASL flow map to MNI152 standard template. Chapter 4 describes the CBF flow map data processing including relative cerebral blood flow calculation, region of interest (ROI) CBF flow extraction and voxel wise analysis of the relation between age and CBF. The result of the relationship between CBF and age is also put here. Chapter 5 includes some discussions, and comparing the CBF results of this study with the CBF results of PET studies.

Chapter 2

Arterial Spin Labeling Image Acquisition

2.1 Ethical Approval and Subjects

173 subjects age ranges from 21 to 80 were participated in this study. There were 107 female subjects and 66 male subjects. The age mean of these 173 subjects was 54, with standard deviation of 16. There were 70 subjects with age less than 55 years old and 103 subjects with age older or equal than 55 years old. The age mean of male subjects was 53, with standard deviation of 15. The age mean of female subjects was 55, with standard deviation of 17. All 173 subjects were relatively healthy without mild cognitive impairment.

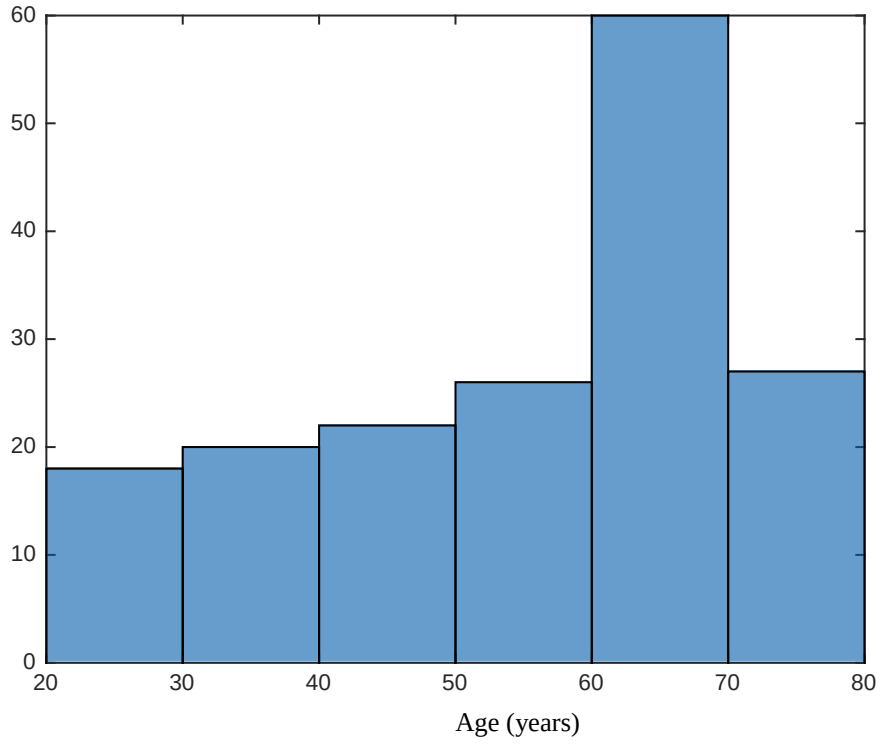

Figure 2-1 Subject age distribution histogram

All subjects signed the informed consent approved by the Institutional Review Boards of the University of Texas Southwestern Medical Center and Texas Health Presbyterian Hospital of Dallas.

2.2 MRI Sequence

2.2.1 Arterial Spin Labeling Image

The whole ASL sequence includes many parts: first is the labeling sequence. Then, a back ground suppression and/or spoiling gradient can be optional. Finally, it is the image acquisition sequence.

First of all, for the labeling sequence, Pseudo-continuous ASL sequence was used for labeling. As mentioned in the introduction part, Pseudo-continuous ASL has higher signal to noise ratio than pulsed labeling ASL, and minimum magnetization transfer effects in comparison with pulsed ASL and continuous ASL. It uses a series of discrete excitation pulses with very short spacing of time to mimic continuous ASL. In this study, the label duration = 1650ms. After 1650 ms of labeling, a single post labeling delay as 1525 ms was given. Post labeling delay (PLD) is the time between the end of the labeling pulse train and image acquisition. As mentioned in the introduction part, it is assumed to be longer than arterial transit time (ATT), but in order to maintain a high signal to noise ratio, PLD is not longer than ATT in all patients. ATT can vary between 500-1500 ms in healthy gray matter and depends on the location of labeling, but in patients with cerebrovascular disease, ATT can be longer than 2000 ms [6]. ATT of white matter is also longer than gray matter. So that as a matter of fact, ATT depends a lot on the situation of vascular system, and also depends a lot on age. The PLD used in this study was just longer than the ATT of healthy gray matter. Only single PLD was used in this experiment, because the true value of ATT was not measured. We just assumed that PLD was longer than ATT.

A control image is the image without labeling sequence. Except for labeling, the control image has the same sequence as the labeled image.

Secondly, no background suppression or vascular crushing gradient was used in this study. In gray matter, in-flow labeled blood only replaces about 1% of the brain water every second, so that the difference between the labeled and control image is less than 1% [6]. ASL is sensitive to noise. If an inversion pulse is applied during the PLD right after the labeled spins signal becomes positive is a good way to reduce the non-ASL signal without affecting ASL signal too much. It improves the signal to noise ratio. But as long as we did not have it, it was fine. A spoiling gradient can get rid of the signal of blood vessels passing the target area without irrigating it. But a spoiling gradient reduces signal to noise ratio, so that it was not used in this study.

Finally, single-shot echo-planar image (EPI) sequence was used for image acquisition. EPI sequence has ultrafast imaging speed. In single-shot EPI, the entire 2D image is acquired using an echo train produced by a single excitation pulse. Single-shot EPI provides good temporal resolution because it obtains snapshot of images and freeze motion. As long as ASL is sensitive to motion artifacts, single-shot EPI is a good option. In this study, EPI sequence imaged each 2D slice in 35 ms. Slice thickness = 5 mm, slice number = 29, voxel size = 3 mm, FOV = 240mm. Each 2D image was a 80×80 matrix. Each 3D image was a 80×80×29 matrix. There were two kinds of TR: 4210.8ms and 4260ms. TE = 14ms, flip angle = 90°. 40 label/control image pairs were acquired for each subject in order to increase signal to noise ratio.

2.2.2 T1 Image

The shape of brains varies among different people. The ASL images acquired have very low spatial resolution. It is difficult to identify where is where, and it is impossible to register these low spatial resolution images into MNI152 standard space.

So, a high-resolution structural image was acquired for each subject on the same day he or she took the ASL images. It is assumed that the ASL images with low spatial resolution can be registered on the T1 image of the same person taken in the same day with only linear registration. High-resolution T1 weighted images were acquired using a magnetization-prepared rapid gradient echo (MPRAGE) sequence. MPRAGE sequence is a robust way to get T1 weighted image with gradient echo. In a spin echo sequence, a relatively short TR and a very short TE is used to get a T1 weighted image. In MPRAGE sequence inversion recovery technique is used to enhance T1 contrast. A non-selective 180 inverse pulse was applied for preparation, then, waited for 868 ms to introduce T1 contrast into the longitudinal magnetization, and then used the turbo field echo (TFE) sequence to fill the k-space fast. In this study, the T1 image acquired with MPRAGE sequence had total scan duration about 4 minutes. Slice number = 160. Slices thickness = 1 mm. Voxel size = 1 mm, FOV=256mm, TR/TE=8.1/3.7 ms. Each 2D image was a 256 × 204 matrix. Each 3D image was a 256×204×160 matrix.

Because Philip MRI machine was used, two formats of images were acquired: PAR/REC and DICOM. In image processing part, only DICOM images were used.

Chapter 3

Arterial Spin Labeling Image Processing

3.1 Preprocess

In this study, FSL was used as tool for image processing. FSL was created by the Analysis Group in Oxford. It is an open source comprehensive library of tools for MRI image processing. It only accepts NFIFTY files, so that all MR images have to be converted from DICOM to NIFTY.

DICOM means digital imaging and communication in medicine. Before 1983, different manufactures of imaging devices had different image formats. For example, Philip MRI machine still has it own image format as PAR/REC. The goal of standardizing the format of medical imaging was achieved in 1983, and DICOM standard was established. Every DICOM file has two components: a header and an image. The image is the 2D image collected by MRI machine. The header includes a description of encoding information in the DICOM image file like the TR/TE, scaling factor, subject information and so on.

The ANALYZE image format was developed at the Mayo Clinic party. ANALYZE separates the header and image part of DICOM into separate files: header files with .hdr extension, and image files with .img extension. But ANALYZE header files contain less information than DICOM header, which incurs ambiguities in interpretation of data. One of the most prominent ambiguity is that the header file of ANALYZE does not contain information about the orientation of image [16].

The newest format using now is NIFTY (neuroimaging informatics technology initiative). It has a .nii extension, and the header and image are merged into the same file. The header information of NIFTY is more extensive than ANALYZE and avoids most of the ambiguities ANALYZE has.

The software dcm2nii, which was created by Chris Rorden and provided under the BSD license, was used to convert the 2320 2D ASL DICOM files into a 4D ASL NIFTY file exactly according to the information in the header file of DICOM. The 160 2D MPRAGE DICOM files were also converted into a 4D T1 NIFTY file using dcm2nii.

During the 2320 2D files were scanned, the subject might move his or her head a bit. Head motion correction is important. Even very small head movement can badly corrupt ASL data because the subtraction of control by labeled for each voxel will be wrong. As mentioned before, the signal differences between the control image and the labeled image is very small, and each voxel is a 3×3×5 mm cube. Without motion correction, the location of voxels of subtraction might be wrong, and this will cause big mistakes. MCFLIRT in FSL tool set was used to do mathematical head motion correction. Of course, any of these corrections depends heavily on the assumption that when the subject moves his or her head, the brain does not change shape or size [16]. MCFLIRT loads the images and defaults to the middle volume as an initial template image. Default setting of MCFLIRT is used in motion correction. MCFLIRT uses its own cost function to do linear registration to that middle volume. First 8mm is used in motion parameters search according to the cost function, then, 2 subsequent searches at 4mm are used to tighter tolerances. All optimizations use tri-linear interpolation [17].

Spatial smoothing involves the application of a filter to the image, which removes high frequency information. It is helpful in increasing signal to noise ratio. Although we are going to lose some high frequency information, by blurring the data across space, it reduces the high frequency noise. By blurring across voxels, it also reduces the mismatch after motion correction. Convoluting the 3D image with 3D Gaussian kernel was used in spatial smoothing. The amount of smoothing is determined by the standard deviation. In image processing, the standard deviation is related to the full width at half-

maximum (FWHM). FWHM is the full width of the distribution at the location where it is half of its maximum. The relationship between standard deviation (σ) and FWHM is: $FWHM = 2\sigma\sqrt{2 \cdot ln2}$. So, a FWHM of 6 mm has σ as 2.54798 mm. The greater the FWHM, the greater the smoothing. In order to reduce noise, a FWHM should not be larger than the active signals detected. Each voxel in this study is a 3×3×5 mm cube, and all the regions of interest (ROIs) are bigger than 6mm cube. Smoothing was done just to ensure the validity of Gaussian random field theory for statistical analysis, so that the FWHM is set about twice the voxel dimensions [18]. So that a Gaussian kernel with FWHM=6 mm was used.

3.2 ASL Perfusion Calculation

There were a lot of assumptions in CBF calculation. First, it was assumed that post label delay was long enough for the whole labeled bolus to get into image plane (post label delay > ATT). And this was not absolutely true. Secondly, it was assumed that all the labeled blood water went into the image plane, and there was no outflow. Finally, it was assumed that only T1 relaxation governed the relaxation of the labeled spins, and the T1 relaxation time of the whole image plane was the same.

It is clear that the way of finding a universal T1 value is not unique. The average T1 of blood and tissue can be used, and the T1 of blood can also be used. Of course the T1 of in vivo blood is also within a range determined by hematocrit fraction and temperature [19]. 1/T1 is linearly dependent on hematocrit within a range. T1 of arterial blood is a bit higher than T1 of venous blood. A value for T1 within that range can be picked, but it is difficult to say which value is the best. In this study, T1 of arterial blood was used. It was according to Dr. Alsop's recommendation [6]. But another study group used T1 of the average of brain tissue (white matter and gray matter) and blood. The result is very different, but it is still difficult to say which way is better.

Labeling efficiency, which is the inversion effect on the labeling plane, is also within a certain range. The labeling efficiency of Pseudo-continuous Arterial spin labeling is not high in compare with pulsed arterial spin labeling. The labeling efficiency is 0.86 ± 0.06 according to a study using phase-contrast velocity MRI to measure the total blood flow to the whole brain. Labeling efficiency depends on flow velocity, so that it depends on subject and physiological condition [8]. In order to follow only 1 recommended standard, 0.85 is used according to Dr. Alsop's recommendation [6].

Blood-brain partition coefficient λ indicates now many mL of blood has the same amount of water as 1 g of tissue. The average of blood-brain partition coefficient of gray matter and white matter was used and it was assumed to be 0.9. Although tissue water density varies among different tissue types, quantification error associated with λ is expected to be less than 10% when using brain-averaged λ [6]. So that it is assumed that blood-brain partition coefficient of the whole brain λ=0.9.

80 3D ASL images were spitted into 40 control images and 40 labeled images. 40 control images were merged together and averaged into a 3D mean control image.

Brain extraction was done on this 3D mean control image using FSL tool: BET. Brain extraction is removing the skull and other non-brain tissue like eyes. BET used tissue segmentation technology to determine the boundary between brain and non-brain tissues.

An ASL difference 4D image, which contains 40 3D (control – labeled) images, was created by voxelwise subtraction of control and labeled for each pair of control and labeled image. This ASL difference 4D image was also averaged into a 3D difference image.

Because in the brain most signal comes from blood, instead of gray and white matter, so that $M_{blood} = M0 \cdot \left(1 - e^{-t/T1_{blood}}\right)$ was used. The time from label to image acquisition was used as t here.

M0 calculation:

$$\mathrm{M0} = \frac{\mathrm{mean(40\ control\ images)}}{1 - \mathrm{e}^{(-\mathrm{TR/T1blood})}}$$

Mean (40 control images): the brain extracted 3D control image was used here.

TR=3665 ms; This TR is the TR for image acquisition. Label duration + post label delay = 3175 ms. The EPI factor for each slice is 35 ms, and there are 29 slices. Because the mean of 29 slices was used in M0 calculation, the PLD of 15th slice was used, which was about 35*14=490 ms. So that T1 decay time was 3665 ms on average.

T1 Blood=1650 ms at 3T. It is the longitudinal relaxation time of blood.

CBF calculation

$$CBF = \frac{(\mathrm{control} - \mathrm{labeled}) \times \lambda}{\mathrm{M0} \times 2 \times \alpha \times (\mathrm{T1\ blood}) \times \mathrm{e}^{\left(-\frac{\mathrm{PLD}}{\mathrm{T1\ blood}}\right)} \times \left(1 - \mathrm{e}^{\left(-\frac{\mathrm{label\ duration}}{\mathrm{T1\ blood}}\right)}\right)} \times 6{,}000{,}000$$

(control - labeled) image: the 3D difference image was used here. All the non-zero voxels of this 3D image was averaged into a number.

α is labeling efficiency (the inversion effect on the labeling plane is not perfectly inverted) =0.85

λ is blood-brain partition coefficient (Conversion factor between gram tissue and mL blood. It indicates how many mL of blood has the same amount of water as 1 g of tissue) =0.9 ml/g

PLD is post label delay, which is adjusted for every slice from the first slice to the last slice. For every slice, 35ms was added, which was the acquisition delay between adjacent slices, because EPI factor is 35ms.

Label duration=1650ms

All the time used here is ms, so that 6000000 was multiplied with the result to convert the units from mL/g/ms to mL/100g/min

Of course, there might also be some T2* relaxation. When TE=10 ms, T2*=47 s. The shorter the TE, the better, because the shorter the TE, the less amount of T2* relaxation. As long as the TE in this experiment is on 14 ms, the T2* relaxation is neglected.

All the parameters and the formula of CBF calculation were according to Dr. Alsop's journal [6].

Table 3-1 Parameters of M0 and CBF Calculation

Parameter	Unit	Explanation
Repetition time (TR) = 3665	ms (millisecond)	Repetition time (TR) is the time interval between successive excitation pulses. This TR is the TR for image acquisition. Label duration + post label delay = 3175 ms. The EPI factor for each slice is 35 ms, and there are 29 slices. Because of the mean, PLD of 15th slice was used, which takes about 35*14=490ms. So that image acquisition has a TR as 3665ms on average.
T1 Blood=1650	ms (millisecond)	T1 is the time constant that describes the recovery of the longitudinal component of net magnetization over time. T1 Blood is the longitudinal relaxation time of blood. For a 3T MRI machine, T1 Blood=1650 ms (Alsop et al., 2014)
α=0.85	No unit	Labeling efficiency (the inversion effect on the labeling plane is not perfectly inversed). One can perform an additional phase-contrast MRI scan to measure the total blood flow to the whole brain to calculate α. (Alsop et al., 2014)
λ=0.9	ml/g	Blood-brain partition coefficient (Conversion factor between gram tissue and mL blood. It indicates how may mL of blood has the same amount of water as 1 g of tissue) (Alsop et al., 2014)
PLD	ms (millisecond)	Post labeling delay which is adjusted for every slice from the first slice to the last slice. For every slice, 35ms was added, which was the acquisition delay between adjacent slices because EPI factor is 35ms.
Label duration	ms (millisecond)	Time of the inverse pulse apply on the labeling plane.

3.3 Cerebral Blood Flow Threshold and Registration

Registration is the process in which, the spatial transformation that maps pints from one image to the corresponding points in another image is found. Three kinds of registration were used in this study. Motion correction is rigid-body linear registration. Aligning the CBF map and T1 structural image is co-registration, which is a standard linear registration with 12 parameters. Registering individual brain into standard template is normalization, which includes both linear and non-linear registration.

The most common templates, which are used for spatial normalization, are known as MNI templates. MNI templates were developed at Montreal Neurological Institute. MNI152 with 1mm voxel size templates were used in this study, including the templates with and without brain extraction.

The 3D mean control image with brain extraction was binarized as a mask. The calculated CBF map was brain extracted with this mask. The calculated CBF can only use mask to do brain extraction, because its resolution was too low to do segmentation.

A threshold was used that all voxels had values less than 0 (mL/100g/minute) were given the value of 0 (mL/100g/minute), and all voxels had values bigger than 300 (mL/100g/minute) were assigned the value of 300 (mL/100g/minute). It is impossible for the labeled image to have a higher voxel value than the control image, so that all voxels of the CBF map should be positive. The CBF should be within a range, but what is the maximum value of CBF is not certain. Some studies used the threshold as 0-200 (mL/100g/minute), while a threshold as 0-300 (mL/100g/minute) was used in this study.

Aligning the CBF map and T1 structural image is called co-registration. Co-registering the CBF flow map and T1 image is critical because the spatial resolution of CBF flow map is poor. After co-registration, the spatial location of the CBF flow map can be identified more correctly. In this study, co-registration was done with the help of the 3D

mean control image. The registration process was that: the brain extracted 3D control image was linearly registered on the brain extracted 3D T1 image and a transformation matrix was generated, then, the threshold CBF flow map was registered on that T1 image using the transformation matrix.

After co-registration, the size and shape of every individual brain was very different from other brains. In order to identify CBF from specific anatomical brain structures, structural brains image have to be registered into specific structural standard brain template. This process is also a registration process, which is called normalization. In this study, MNI152 T1 1mm brain was used as the structural standard brain template. The T1 structural image was registered on MNI152_1mm template. The normalization includes 2 steps: linear registration and non-linear registration. The first step was finding the linear transformation matrix that aligns the T1 image to MNI152 template as closely as possible and a transformation matrix was generated. This was an affine transformation matrix with 12 parameters (3 translations, 3 rotations, 3 zooms and 3 shears). After affine transformation, T1 and MNI152 template had roughly the same size, orientation and location on x, y, z dimensions. Only local stretching and shrinking were needed. So, in the second step, a non-linear transformation was performed. Of course, there are infinite numbers of way to do non-linear registration. FSL tool: FNIRT was used in doing non-linear registration. After non-linear registration, a warp field was created by FNIRT. The flow map was registered on MNI152_1mm template according to the warp field created by FNIRT.

Chapter 4

Data Processing and Results

4.1 Data Processing and analysis

Regional cerebral blood flow (rCBF) was used to indicate changes in blood flow.

rCBF = (CBF of each voxel) / (mean of non-zero voxels of whole brain CBF)

Voxelwise analysis was used to analyze the relationship between age and CBF in every region. FSL tool: FEAT general linear model was used in voxelwise analysis. The MNI152 registered CBF flow map of 173 subjects was merged into a 4D file as a group. The rCBF flow map, which was generated from CBF flow map, was also merged into a 4D file as a group. A design matrix was created by FEAT according to the age of each subject in the group as figure 4-1 showed. It only included one group and concerned about only one event, which was age. Two single sample t-tests were set. One contrast was testing the p-value of the CBF of a voxel positively correlated with age. The other contrast was testing the p-value of the CBF of a voxel negatively correlated with age. FSL tool: RANDOMISE was used to generate 5000 permutations of the data to test against the null distribution. The age data was demeaned by the program to test the correlation of CBF in each voxel and age. MNI152 brain extracted binary mask was used in the voxelwise analysis, so that any voxel outside of the brain was not analyzed. Both CBF and rCBF data of the 173 subjects were merged into one group.

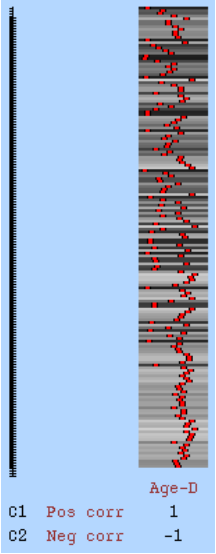

Figure 4-1 Design Matrix of Voxelwise Analysis

Region of interest flow extraction was important to find out regional effects of age on CBF. First, 16 regional masks were created using Harvard-Oxford subcortical structural atlas and threshold and binalized them. CBF were extracted from the whole brain and 16 region of interest including Frontal lobe cortex; Occipital lobe cortex; Parietal lobe cortex; Temporal lobe cortex; Cerebral Cortex left; Cerebral Cortex right; White matter left; White matter right; Hippocampus left; Hippocampus right; Prefrontal cortex left; Prefrontal cortex right; Cingulate Cortex Posterior left; Cingulate Cortex Posterior right; Precuneous Cortex left; Precuneous Cortex right.

Both CBF flow map and rCBF flow map had regional flow extracted from these 16 regions of interest.

4.2 Results

Subject number was 173, with 107 female subjects and 66 male subjects. The age of these 173 subjects ranged from 21 to 80, with mean = 54.2890, and standard deviation=16.1425. There were 70 subjects with age less than 55 years old and 103 subjects with age bigger or equal than 55 years old.

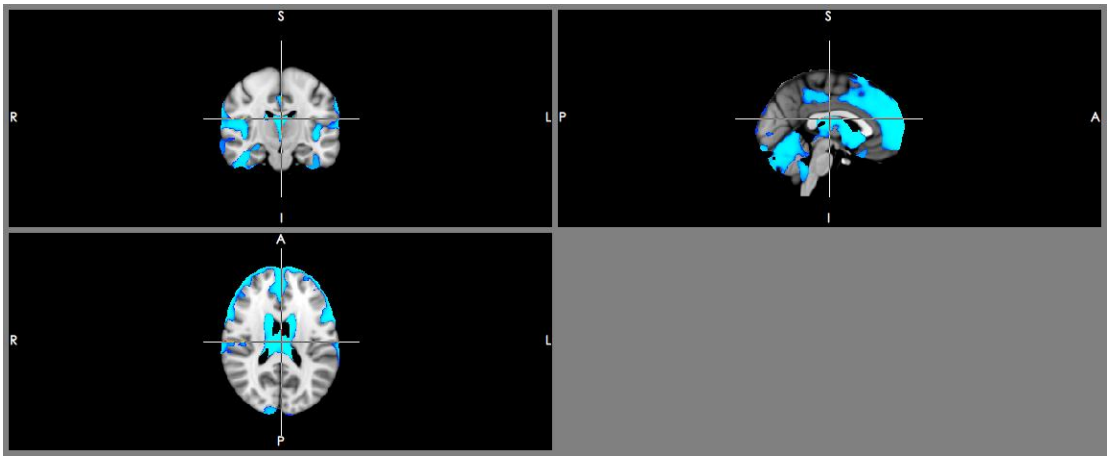

Figure 4-2 The Voxelwise Analysis Result of CBF ($p<0.05$) (red is positive correlation, blue is negative correlation)

Table 4-1 Voxel count of CBF negative correlated with age in 16 ROI

Region	CBF_negative
Frontal_lobe	77575
Occipital lobe	4394
Parietal lobe	11622
Temporal lobe	43798
Cerebral Cortex left	71769
Cerebral Cortex right	100480
White matter left	6453
White matter right	10908
Hippocampus left	30
Hippocampus right	1135
Prefrontal left	9650
Prefrontal right	15408
Cingulate Cortex Posterior left	935
Cingulate Cortex Posterior right	1233
Precuneus Cortex left	263
Precuneus Cortex right	409

There is no voxel positively correlated with age. According to figure 4-2 and table 4-1, frontal lobe is the lobe most negatively correlated with age within the 4 lobes. For regional, right prefrontal cortex is the region most negatively correlated with age. Right side of the hemisphere of the brain is more negatively correlated with age than the left hemisphere.

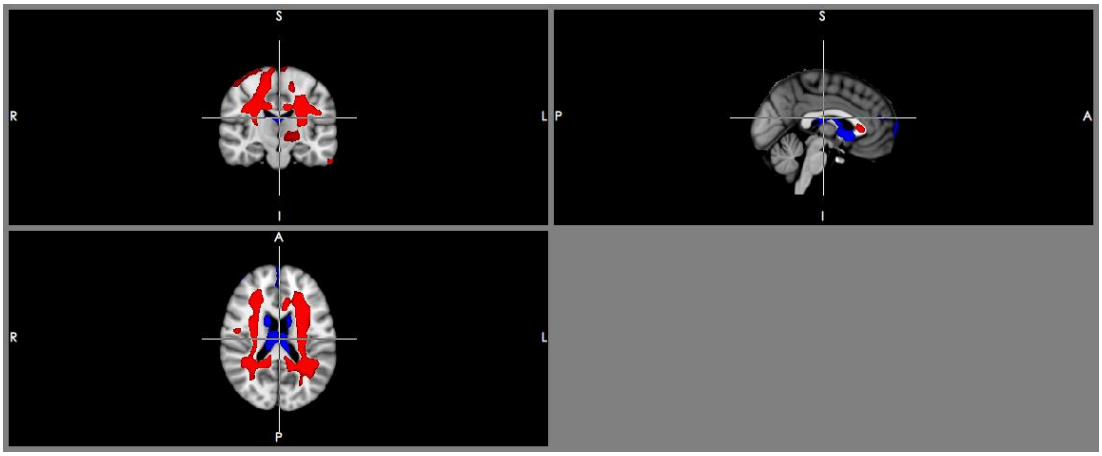

Figure 4-3 The Voxelwise Analysis Result of rCBF ($p<0.05$) (red is positive correlation, blue is negative correlation)

Table 4-2 Voxel count of rCBF positive/negative correlated with age in 16 ROI

Region	rCBF_possitive	rCBF_negative
Frontal_lobe	3047	1255
Occipital lobe	2083	0
Parietal lobe	3427	0
Temporal lobe	1864	273
Cerebral Cortex left	3325	994
Cerebral Cortex right	4781	1656
White matter left	81453	1466
White matter right	61679	1200
Hippocampus left	0	0
Hippocampus right	0	0
Prefrontal left	0	60
Prefrontal right	0	473
Cingulate Cortex Posterior left	0	0
Cingulate Cortex Posterior right	0	0
Precuneus Cortex left	0	0
Precuneus Cortex right	0	0

According to figure 4-3 and table 4-2, prefrontal cortex is the only place where rCBF is only negatively correlated with age. White matter is the tissue seems to contain more voxels positively correlated with age than other tissue.

Table 4-3 Mean Resulting CBF and rCBF in Whole Brain and 16 ROI

	Mean CBF (mL/100g/min)	
Brain region	CBF	rCBF
Whole brain	43.39 ± 8.44	
Frontal_lobe	42.11 ± 9.1	1.21 ± 0.11
Occipital lobe	53.45 ± 11.82	1.54 ± 0.15
Parietal lobe	48.77 ± 10.3	1.4 ± 0.13
Temporal lobe	45.19 ± 8.98	1.3 ± 0.11
Cerebral Cortex left	47.43 ± 9.23	1.37 ± 0.09
Cerebral Cortex right	48.93 ± 10.19	1.41 ± 0.09
White matter left	34.7 ± 6.66	1 ± 0.09
White matter right	34.82 ± 7.36	1 ± 0.1
Hippocampus left	56.17 ± 11.28	1.63 ± 0.22
Hippocampus right	55.31 ± 12.26	1.6 ± 0.25
Prefrontal left	45.43 ± 10.39	1.31 ± 0.15
Prefrontal right	44.49 ± 10.69	1.28 ± 0.17
Cingulate Cortex Posterior left	70.11 ± 16.7	2.02 ± 0.31
Cingulate Cortex Posterior right	72.99 ± 17.07	2.1 ± 0.31
Precuneus Cortex left	58.5 ± 13.81	1.68 ± 0.21
Precuneus Cortex right	60.41 ± 14.1	1.74 ± 0.21

Table 4-4 The Correlation Coefficient of CBF/rCBF with Age Whole Brain and 16 ROI

Brain region	CBF	rCBF
Whole brain	-0.2355	
Frontal_lobe	-0.3035	-0.3099
Occipital lobe	-0.177	-0.0189
Parietal lobe	-0.1931	-0.0312
Temporal lobe	-0.2958	-0.2556
Cerebral Cortex left	-0.2656	-0.1797
Cerebral Cortex right	-0.2729	-0.3192
White matter left	0.0009	0.4263
White matter right	-0.0327	0.2817
Hippocampus left	-0.2638	-0.0892
Hippocampus right	-0.3005	-0.193
Prefrontal left	-0.2916	-0.2227
Prefrontal right	-0.3108	-0.2731
Cingulate Cortex Posterior left	-0.2316	-0.1074
Cingulate Cortex Posterior right	-0.266	-0.1709
Precuneus Cortex left	-0.1802	-0.0151
Precuneus Cortex right	-0.1982	-0.0722

According to table 4-4, white matter does not seem to be correlated with age. Right prefrontal cortex and right hippocampus seem to be more correlated with age than other areas.

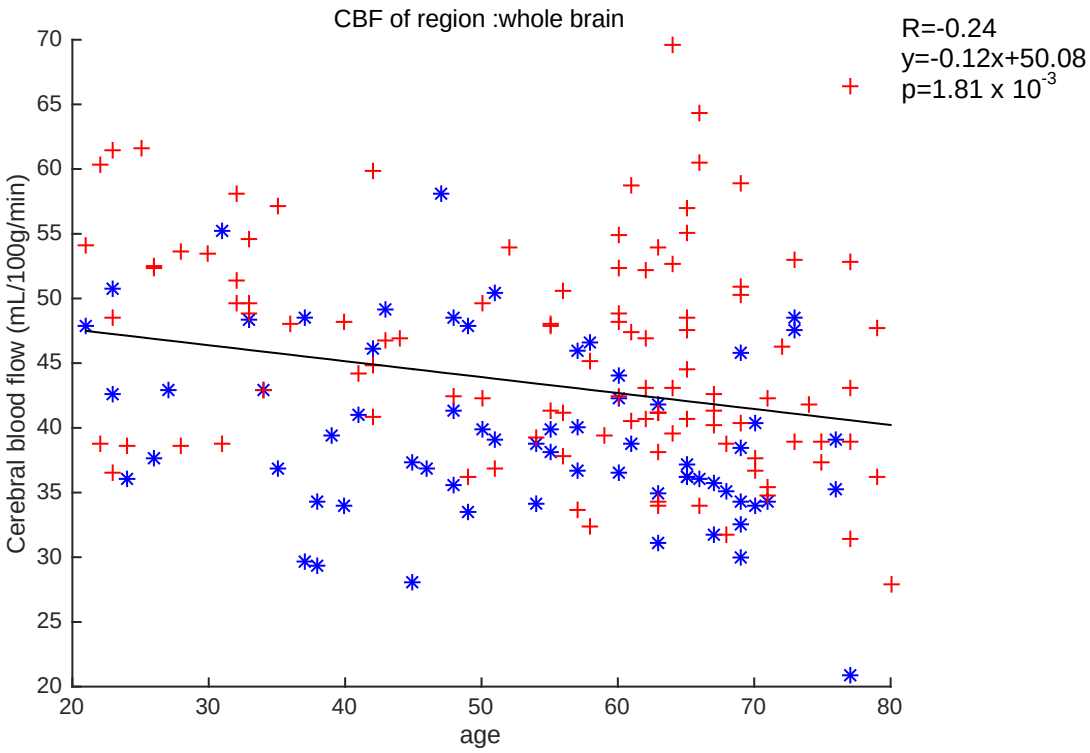

Figure 4-4 CBF of whole brain (blue '*' represents male, red '+' represents female)

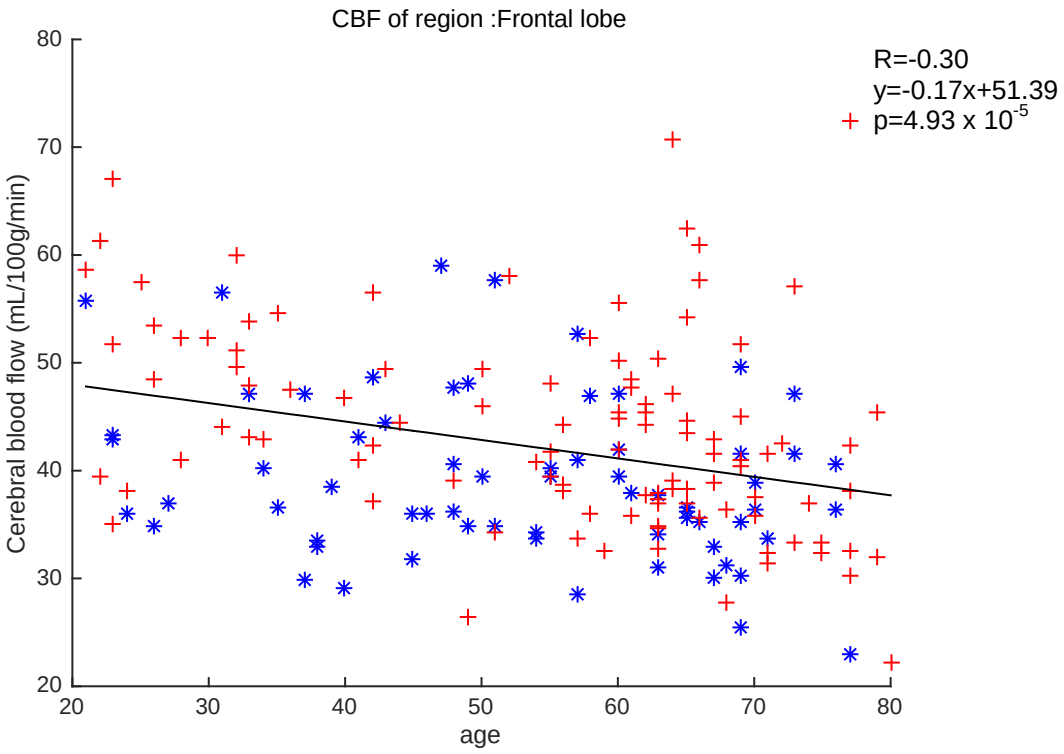

Figure 4-5 CBF of Frontal lobe (blue '*' represents male, red '+' represents female)

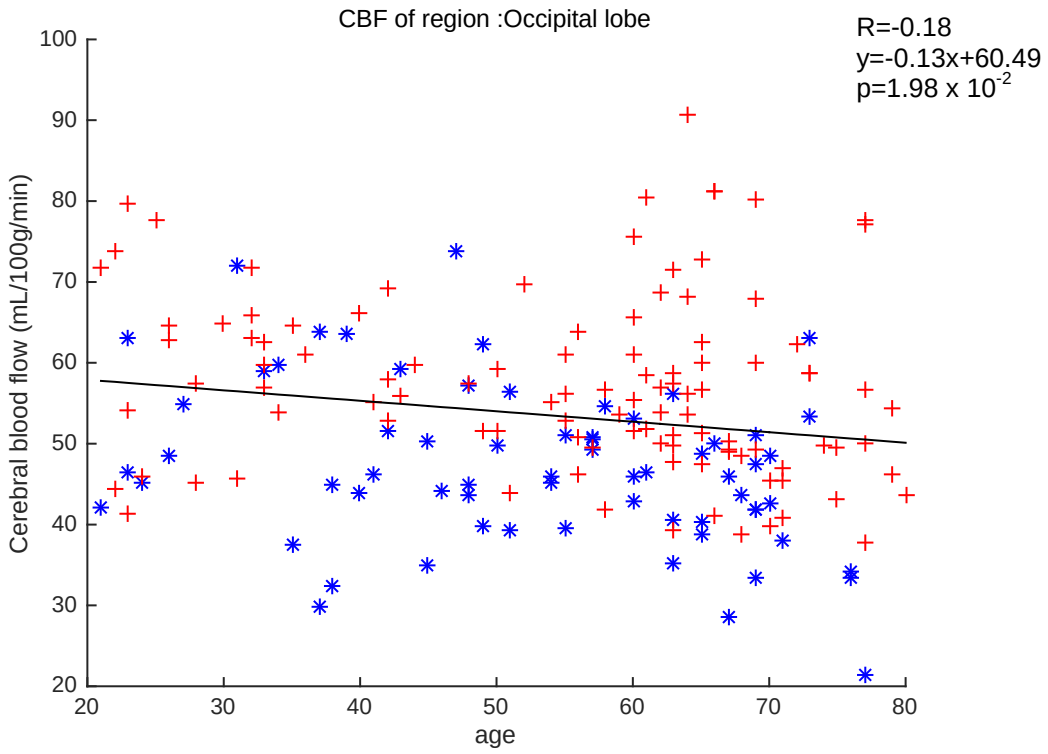

Figure 4-6 CBF of Occipital lobe (blue '*' represents male, red '+' represents female)

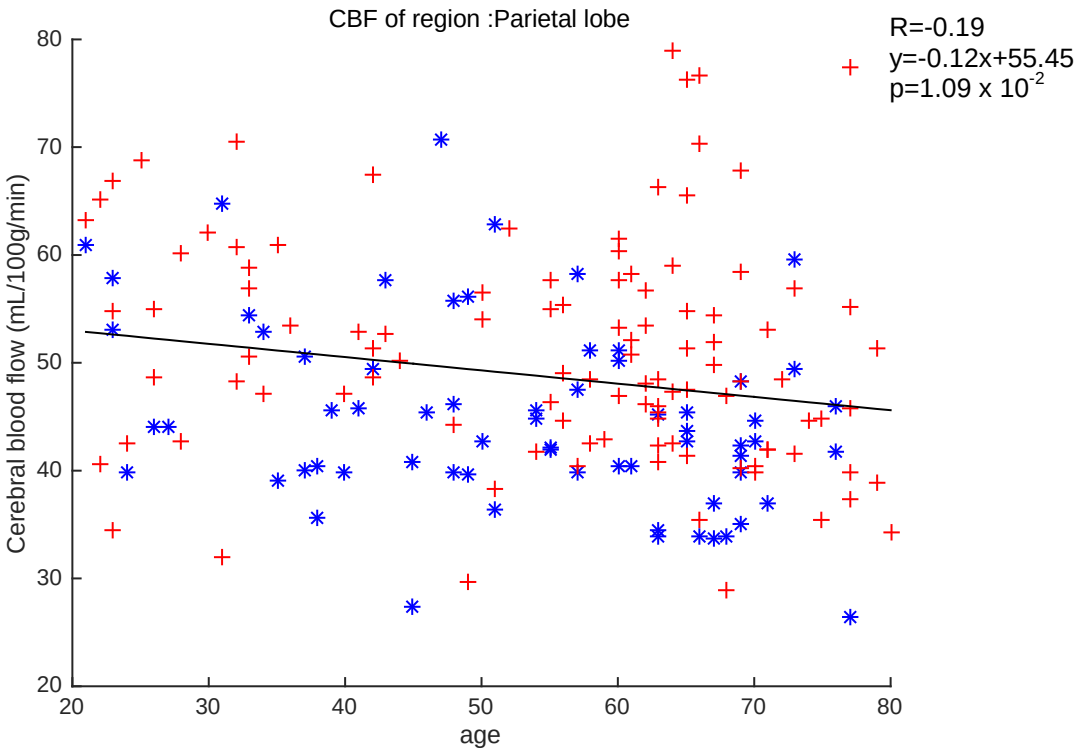

Figure 4-7 CBF of Parietal lobe (blue '*' represents male, red '+' represents female)

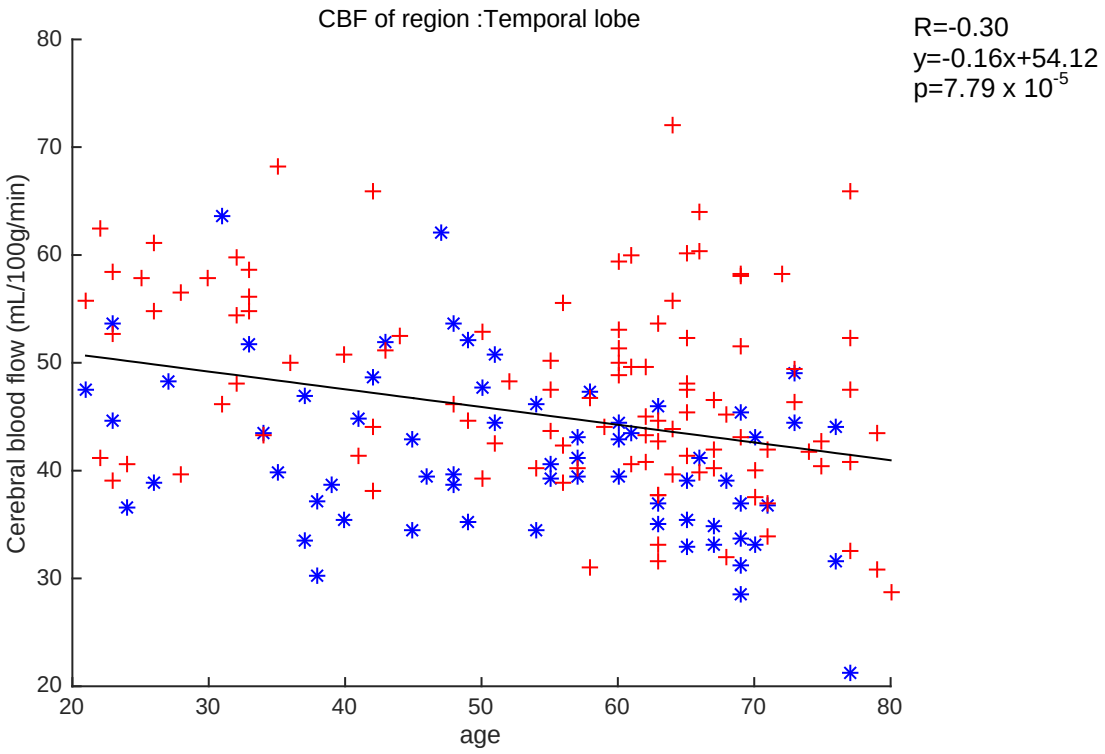

Figure 4-8 CBF of Temporal lobe (blue '*' represents male, red '+' represents female)

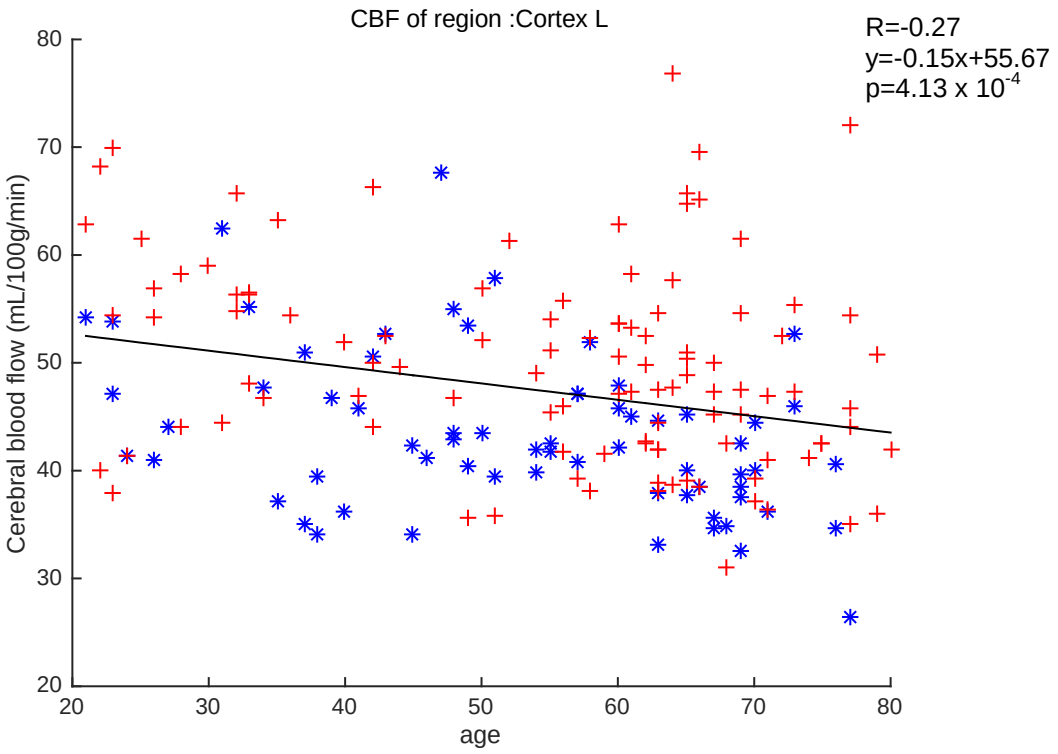

Figure 4-9 CBF of Cerebral Cortex Left (blue '*' represents male, red '+' represents female)

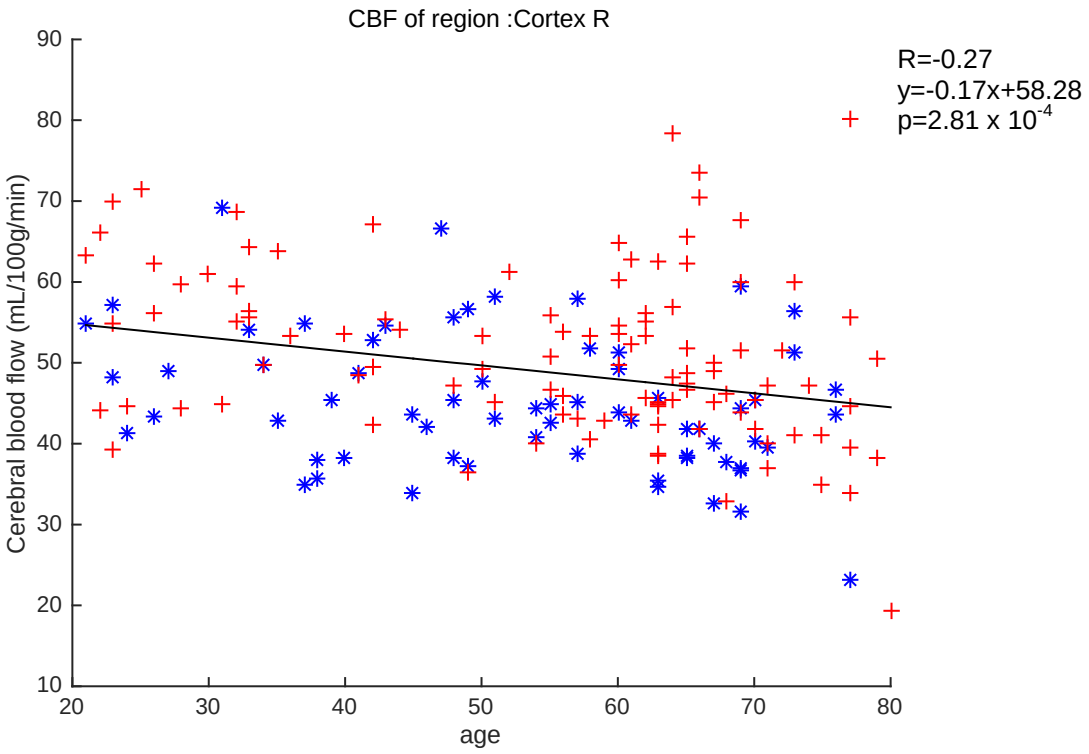

Figure 4-10 CBF of Cerebral Cortex Right (blue '*' represents male, red '+' represents female)

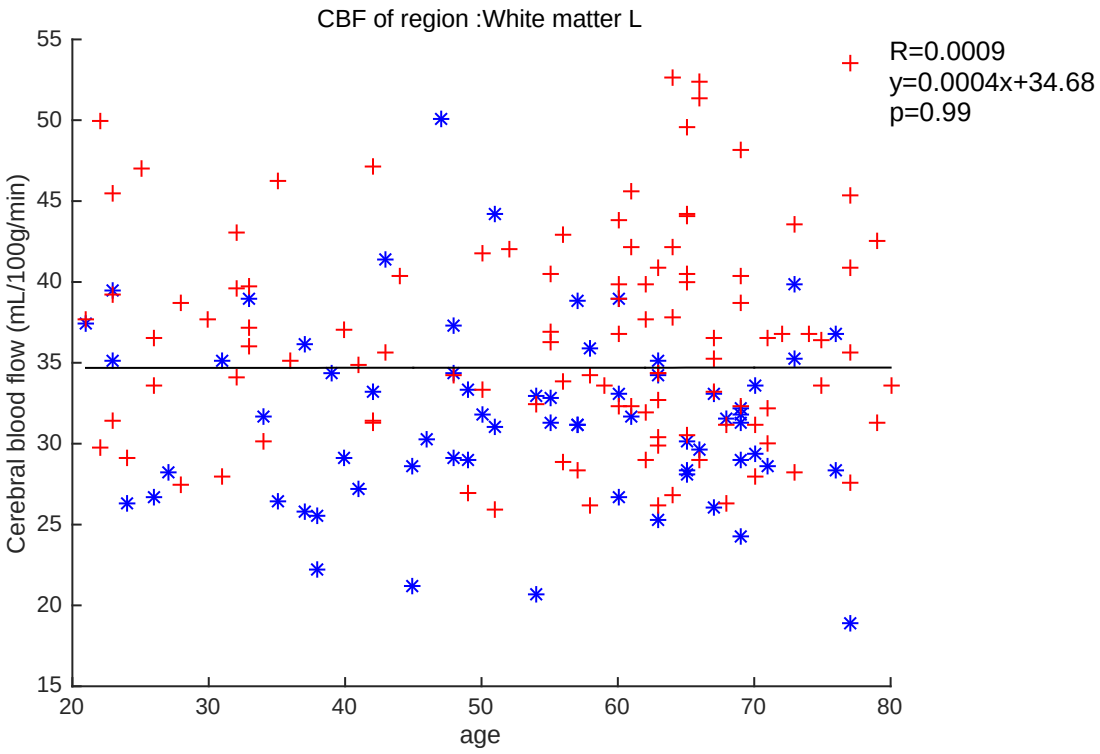

Figure 4-11 CBF of White Matter Left (blue '*' represents male, red '+' represents female)

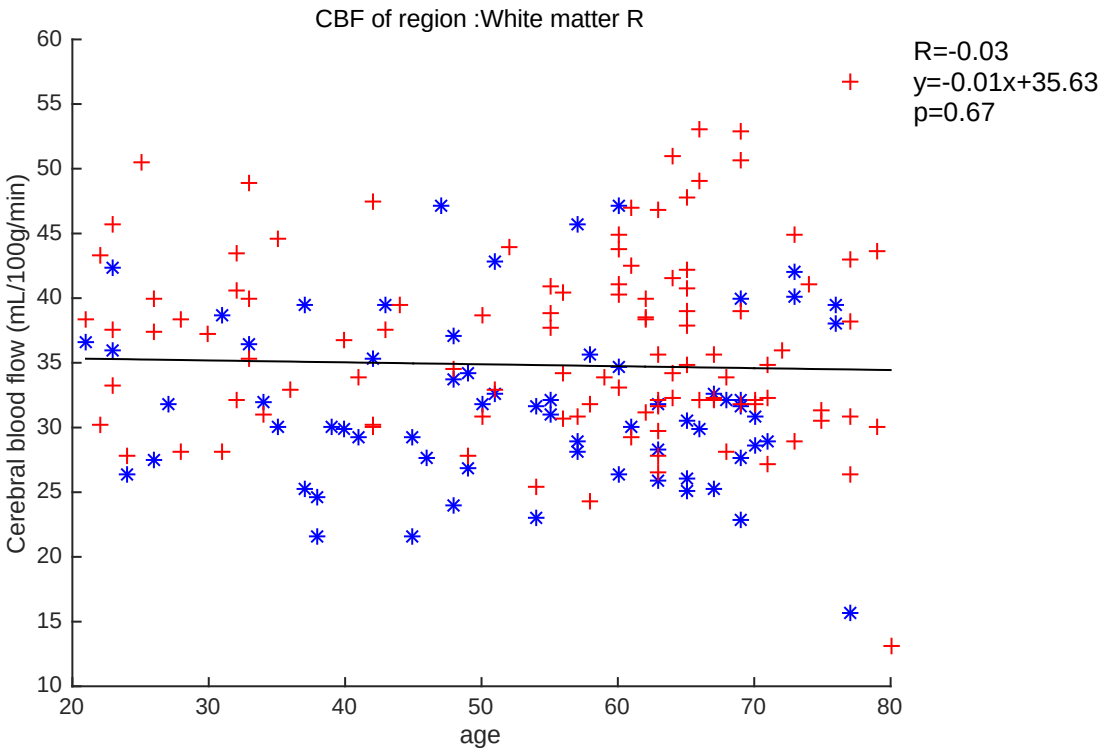

Figure 4-12 CBF of White Matter Right (blue '*' represents male, red '+' represents female)

Hippocampus

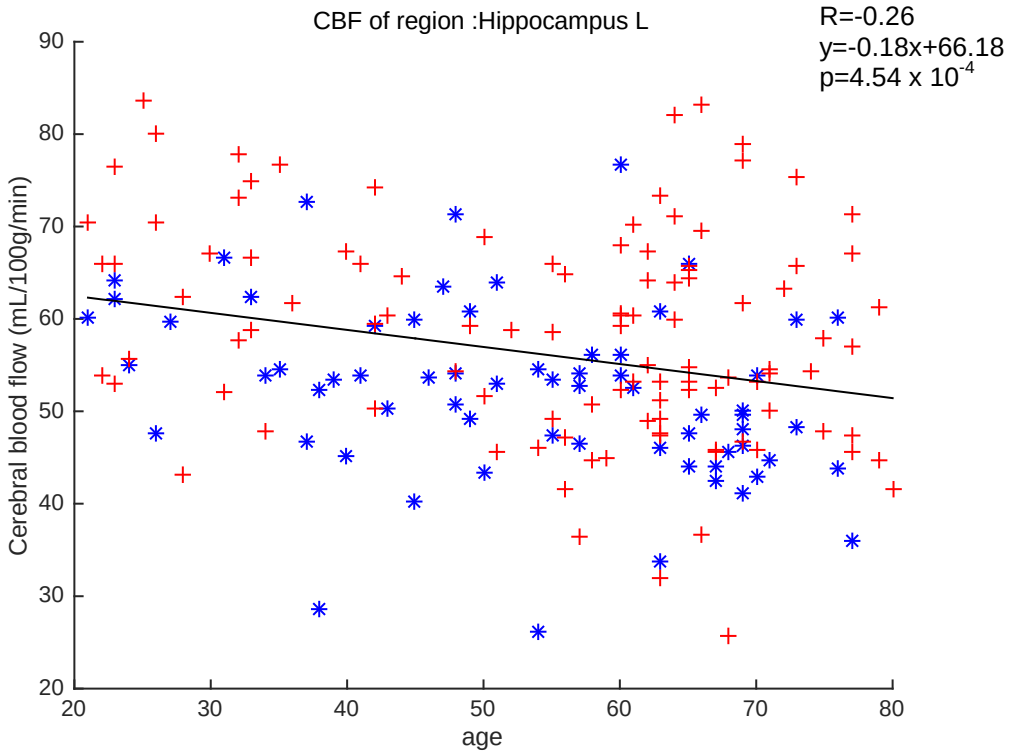

Figure 4-13 CBF of Hippocampus Left (blue '*' represents male, red '+' represents female)

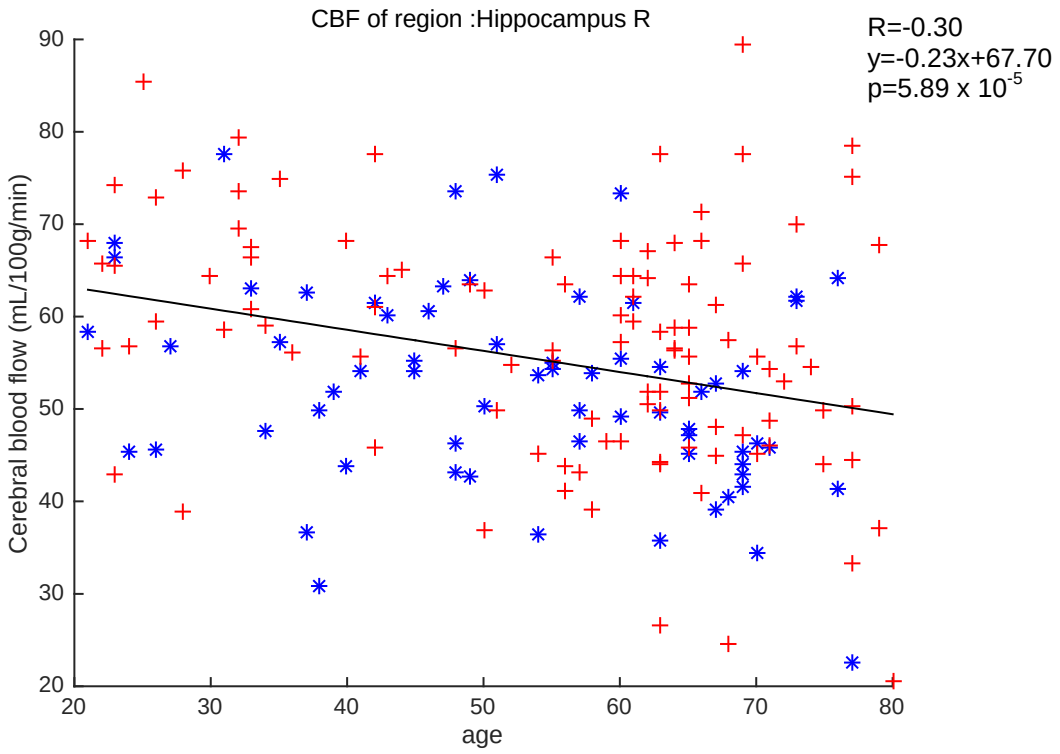

Figure 4-14 CBF of Hippocampus Right (blue '*' represents male, red '+' represents female)

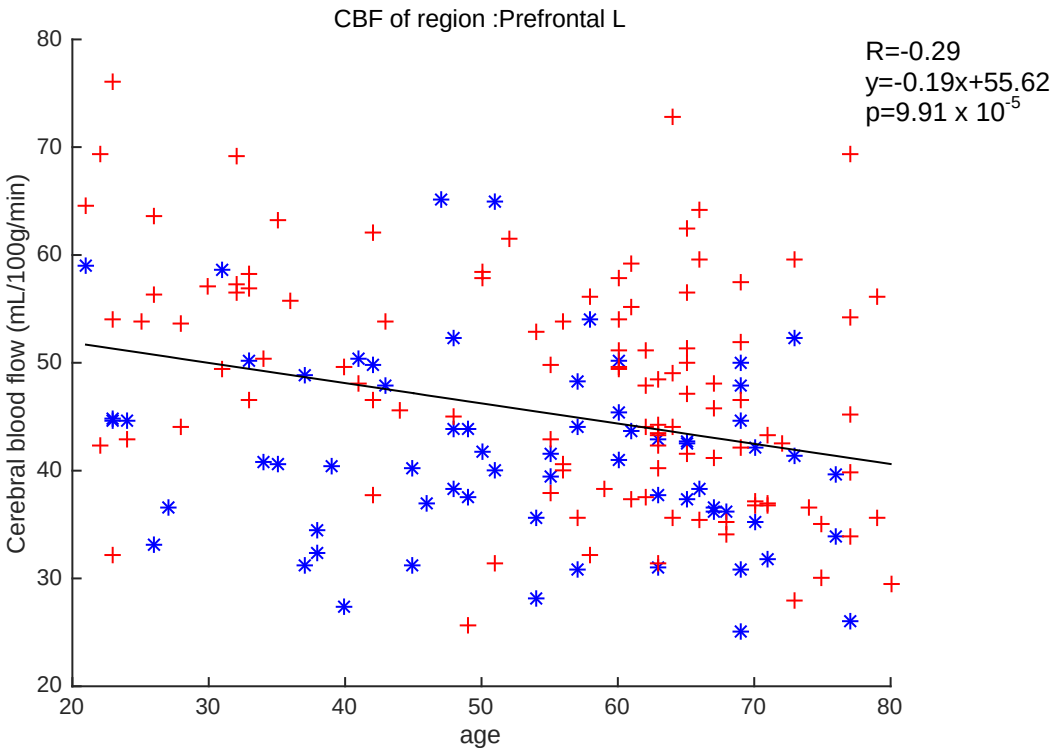

Figure 4-15 CBF of Prefrontal Cortex Left (blue '*' represents male, red '+' represents female)

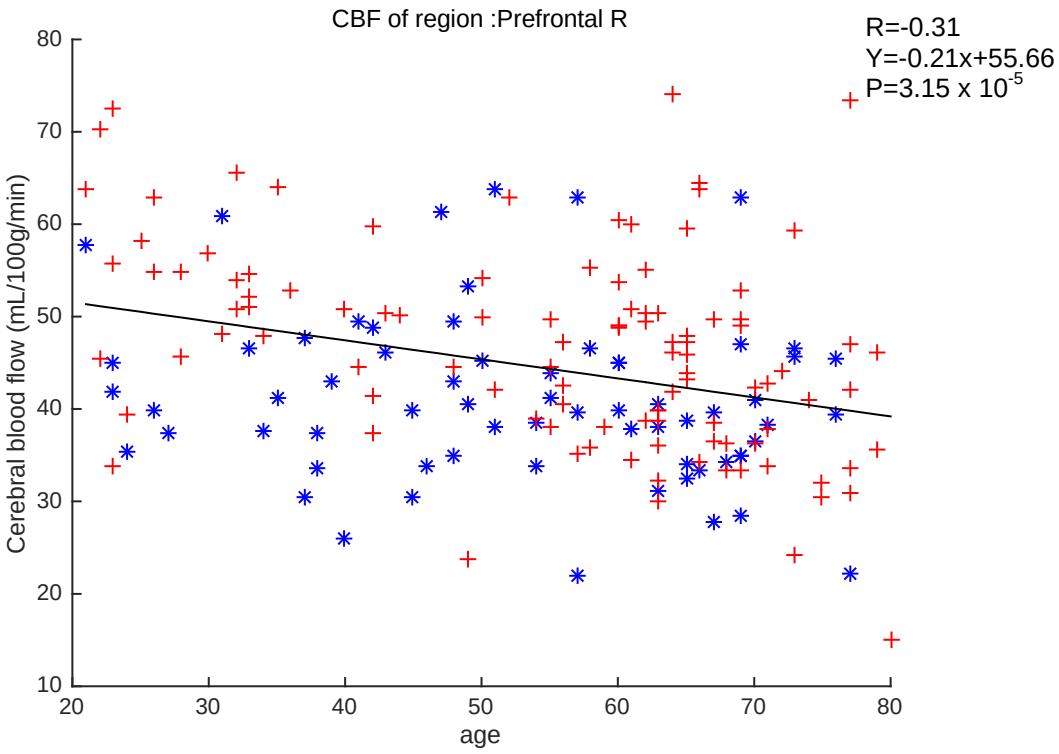

Figure 4-16 CBF of Prefrontal Cortex Right (blue '*' represents male, red '+' represents female)

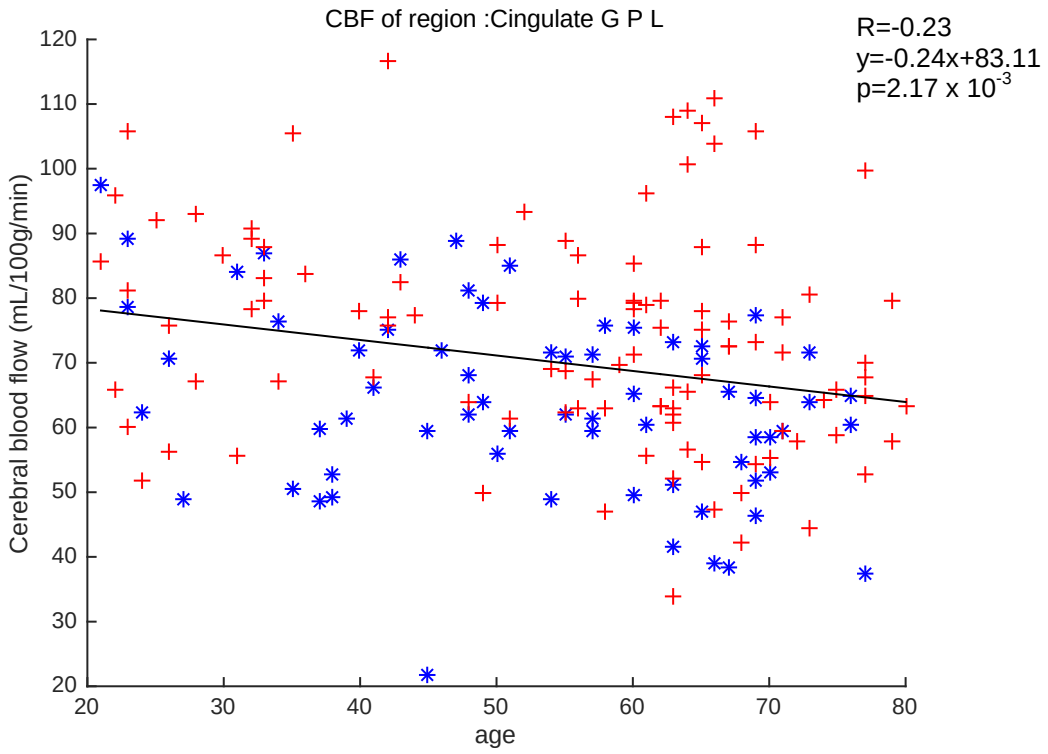

Figure 4-17 CBF of Cingulate Cortex Posterior Left (blue '*' represents male, red '+' represents female)

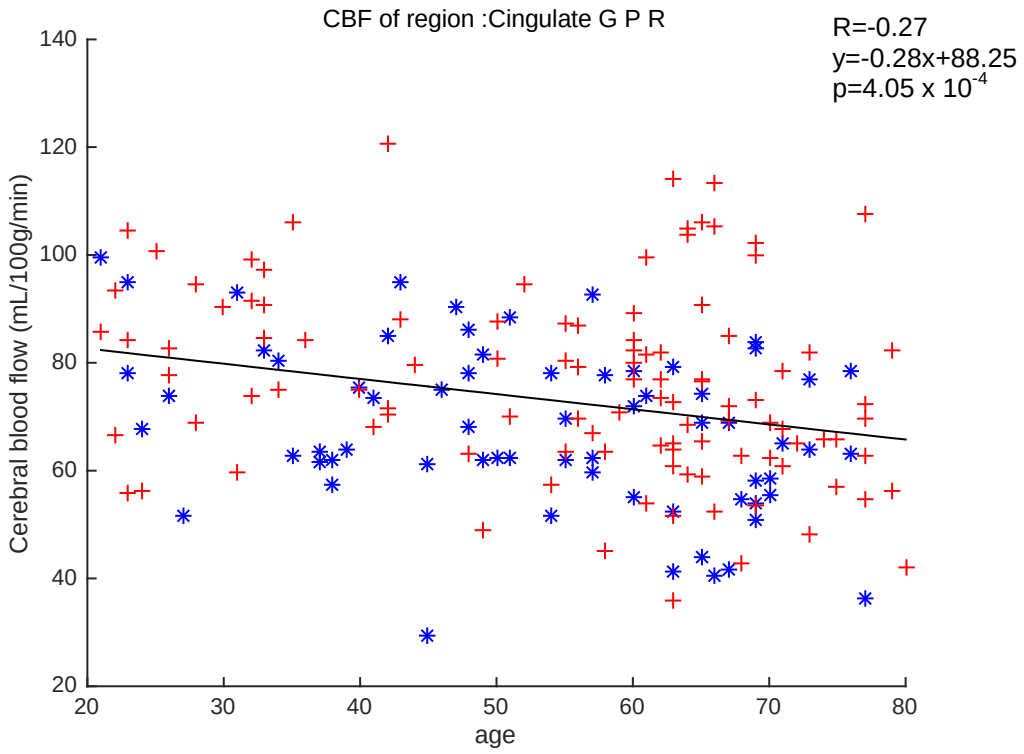

Figure 4-18 CBF of Cingulate Cortex Posterior Right (blue '*' represents male, red '+' represents female)

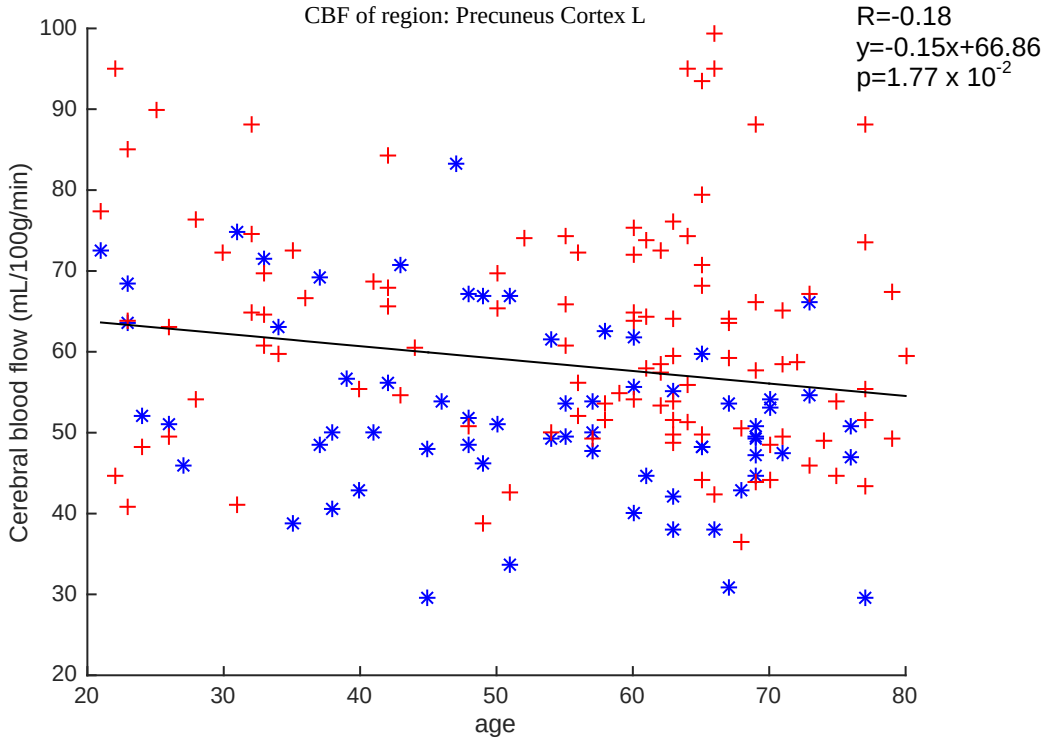

Figure 4-19 CBF of Precuneus Cortex Left (blue '*' represents male, red '+' represents female)

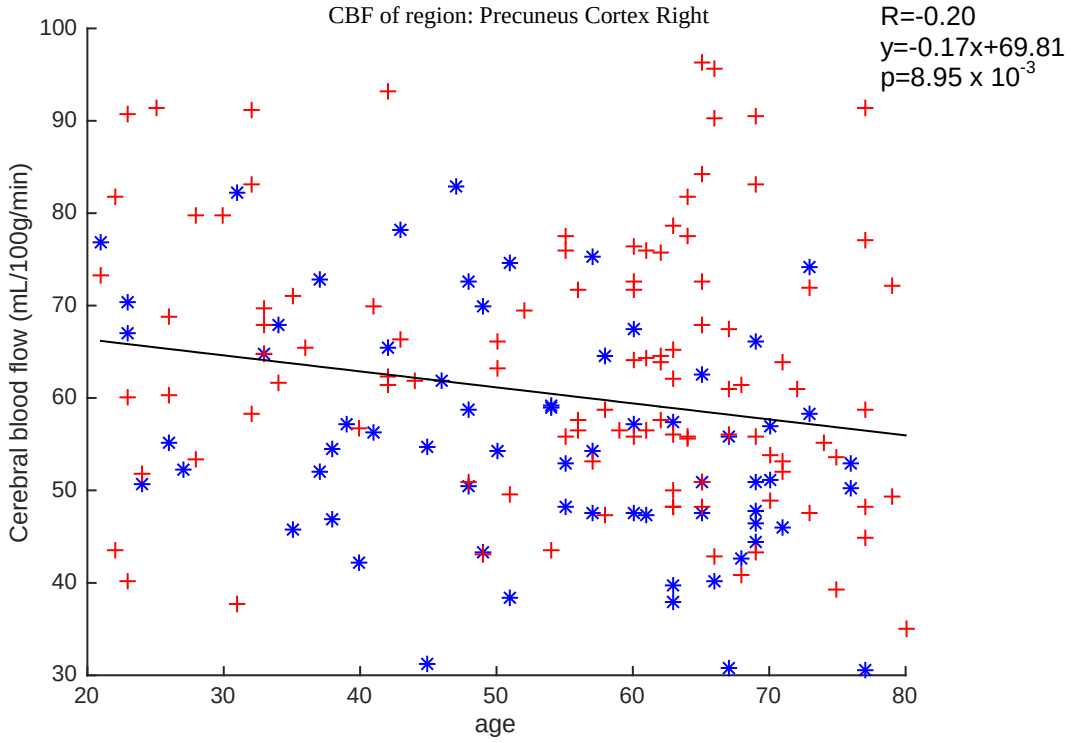

Figure 4-20 CBF of Precuneus Cortex Right (blue '*' represents male, red '+' represents female)

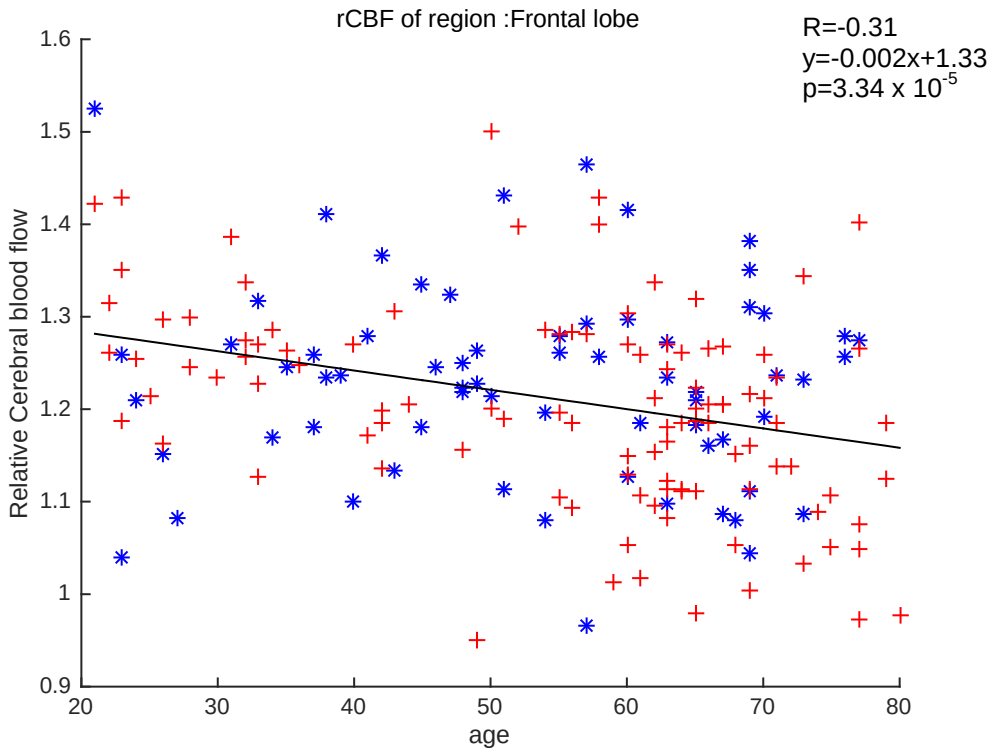

Figure 4-21 rCBF of Frontal lobe (blue '*' represents male, red '+' represents female)

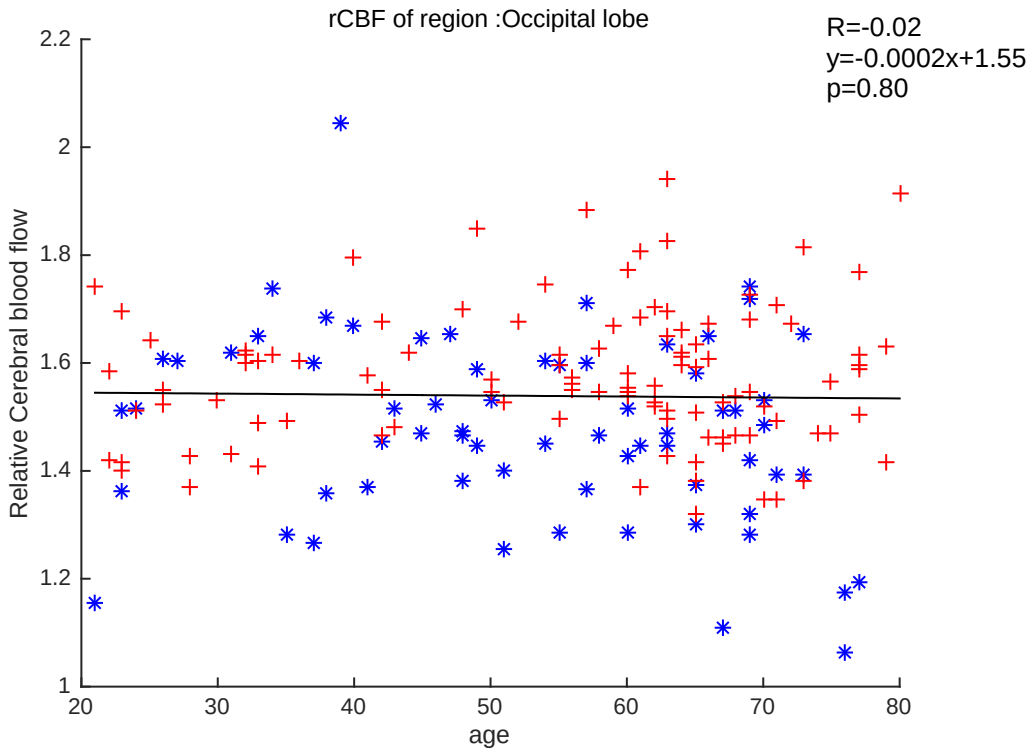

Figure 4-22 rCBF of Occipital lobe (blue '*' represents male, red '+' represents female)

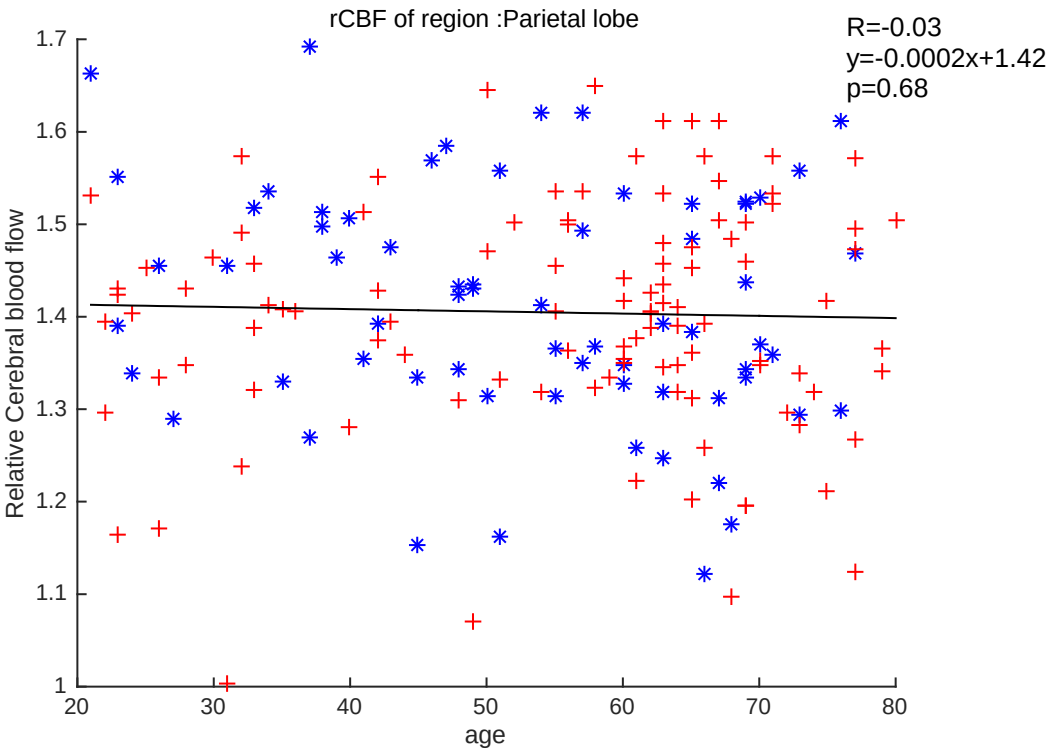

Figure 4-23 rCBF of Parietal lobe (blue '*' represents male, red '+' represents female)

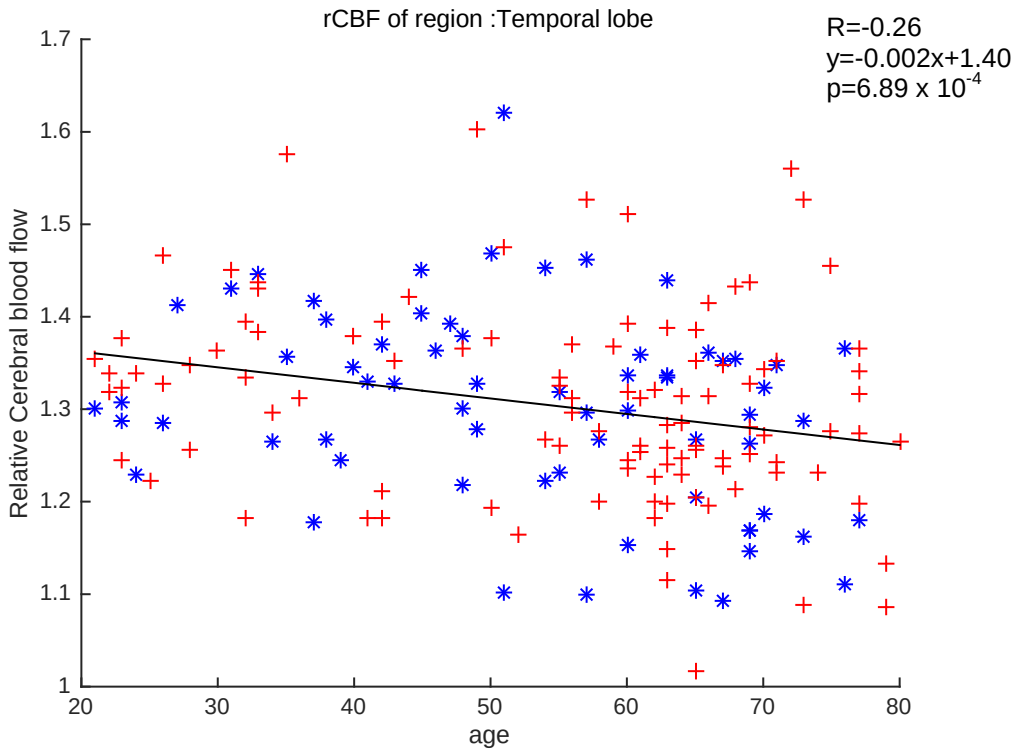

Figure 4-24 rCBF of Temporal lobe (blue '*' represents male, red '+' represents female)

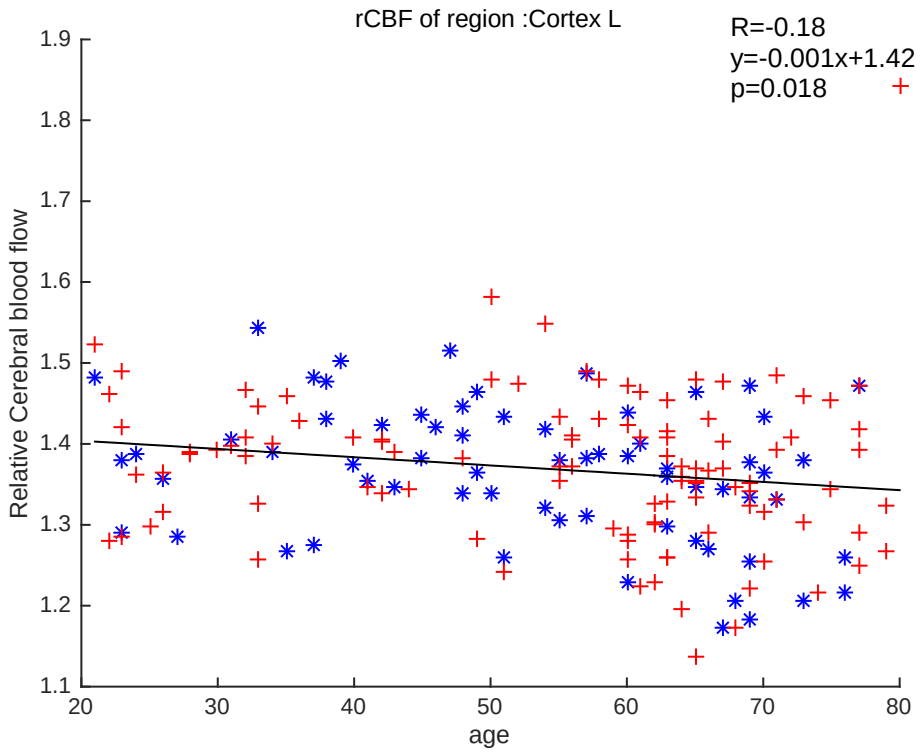

Figure 4-25 rCBF of Cerebral Cortex Left (blue '*' represents male, red '+' represents female)

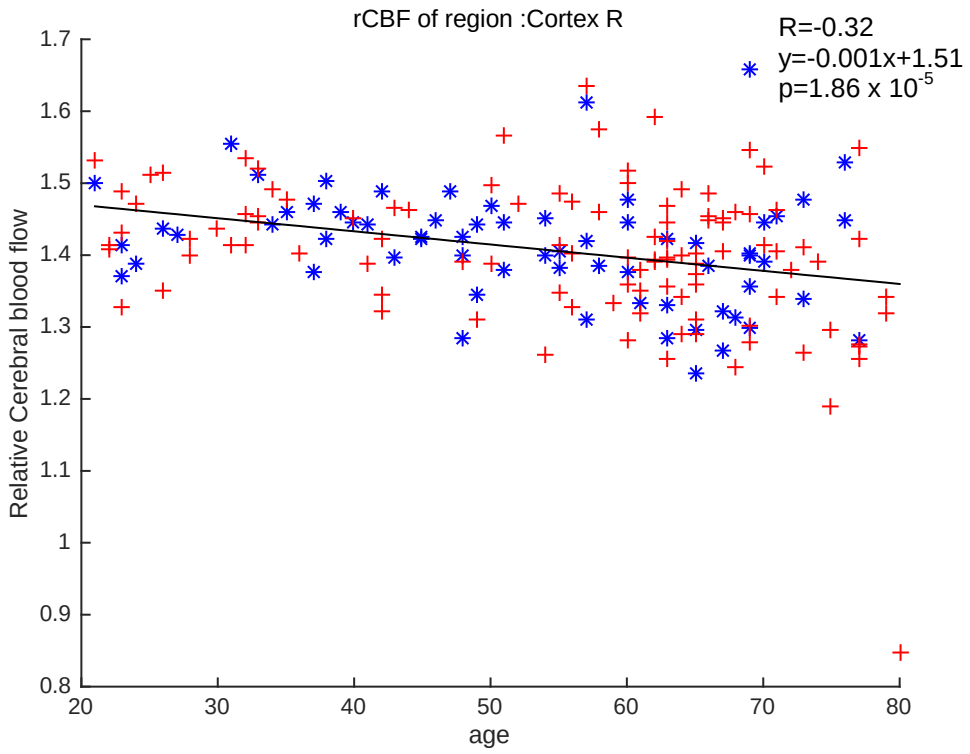

Figure 4-26 rCBF of Cerebral Cortex Right (blue '*' represents male, red '+' represents female)

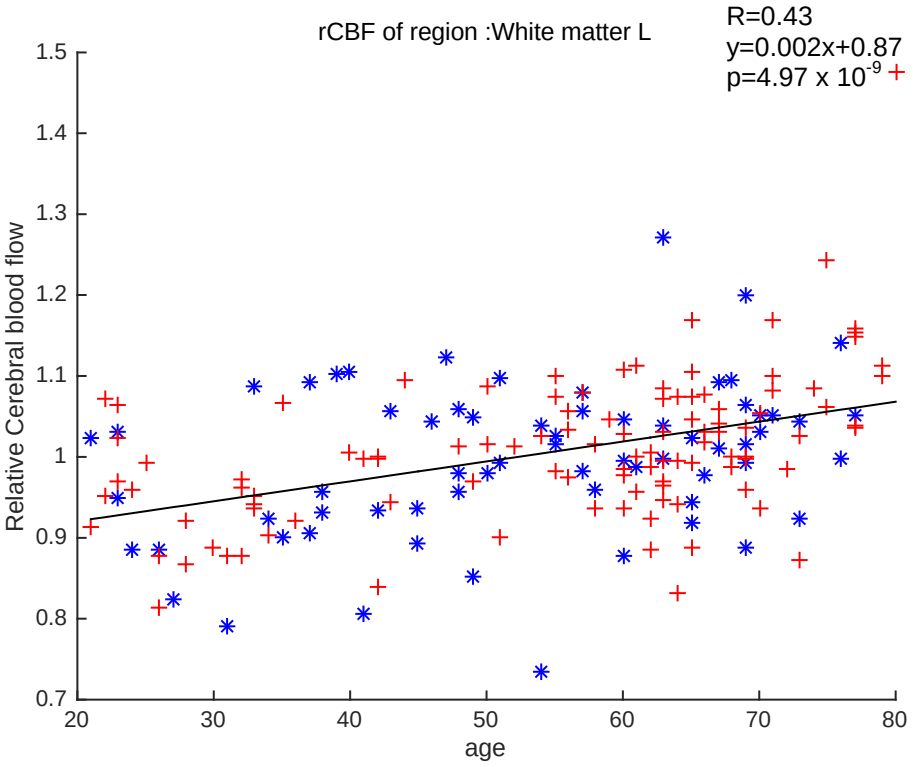

Figure 4-27 rCBF of White Matter Left (blue '*' represents male, red '+' represents female)

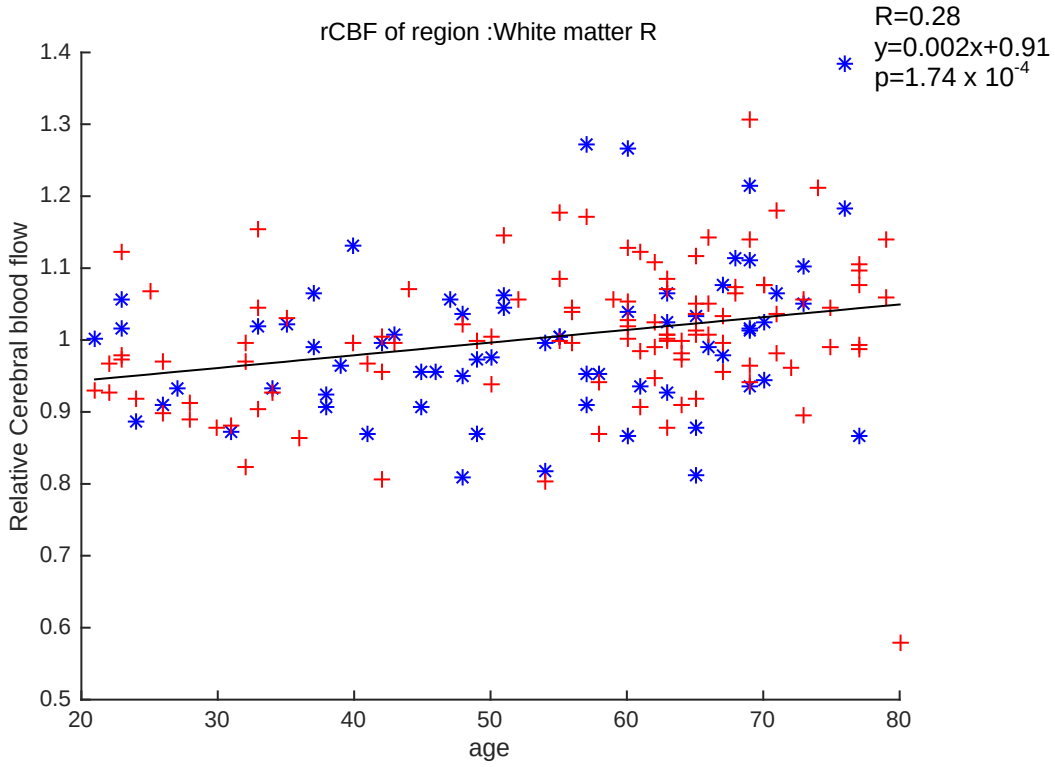

Figure 4-28 rCBF of White Matter Right (blue '*' represents male, red '+' represents female)

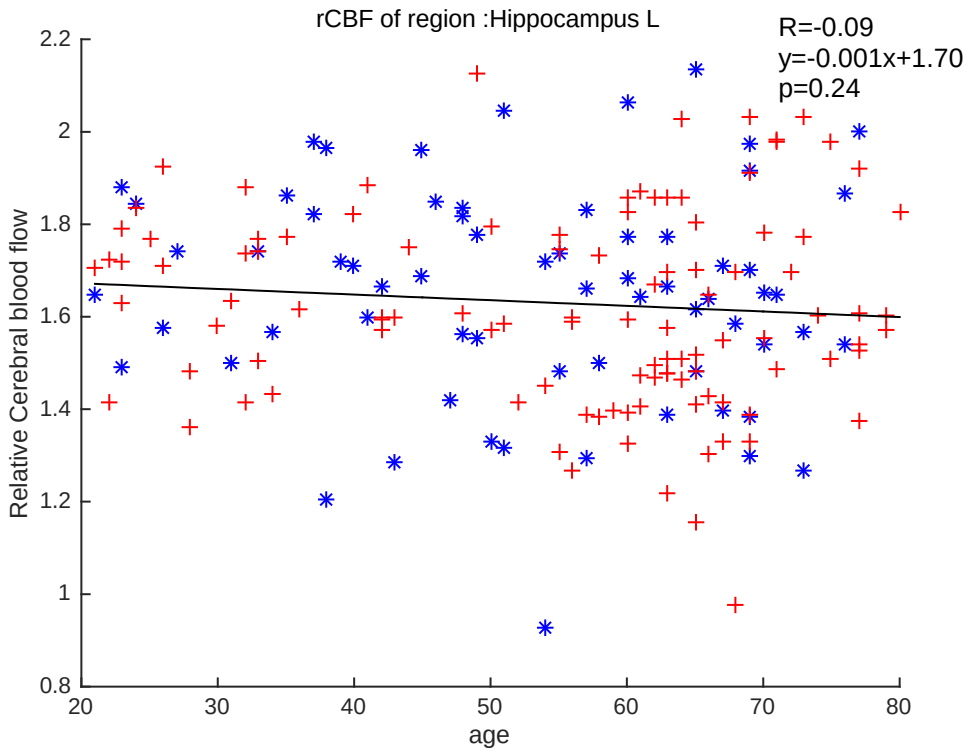

Figure 4-29 rCBF of Hippocampus Left (blue '*' represents male, red '+' represents female)

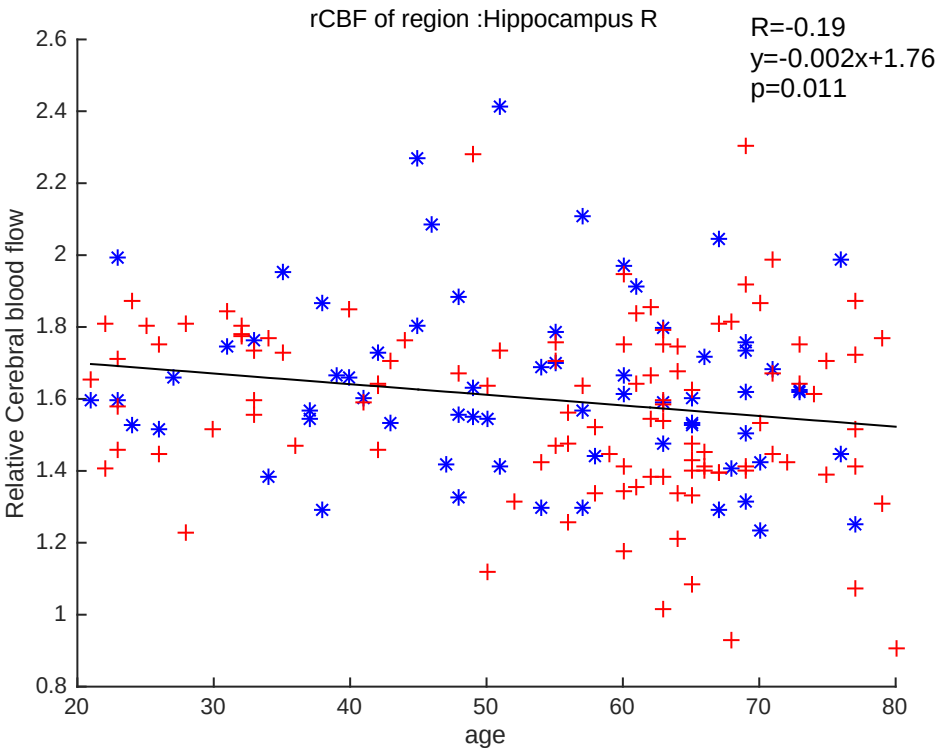

Figure 4-30 rCBF of Hippocampus Right (blue '*' represents male, red '+' represents female)

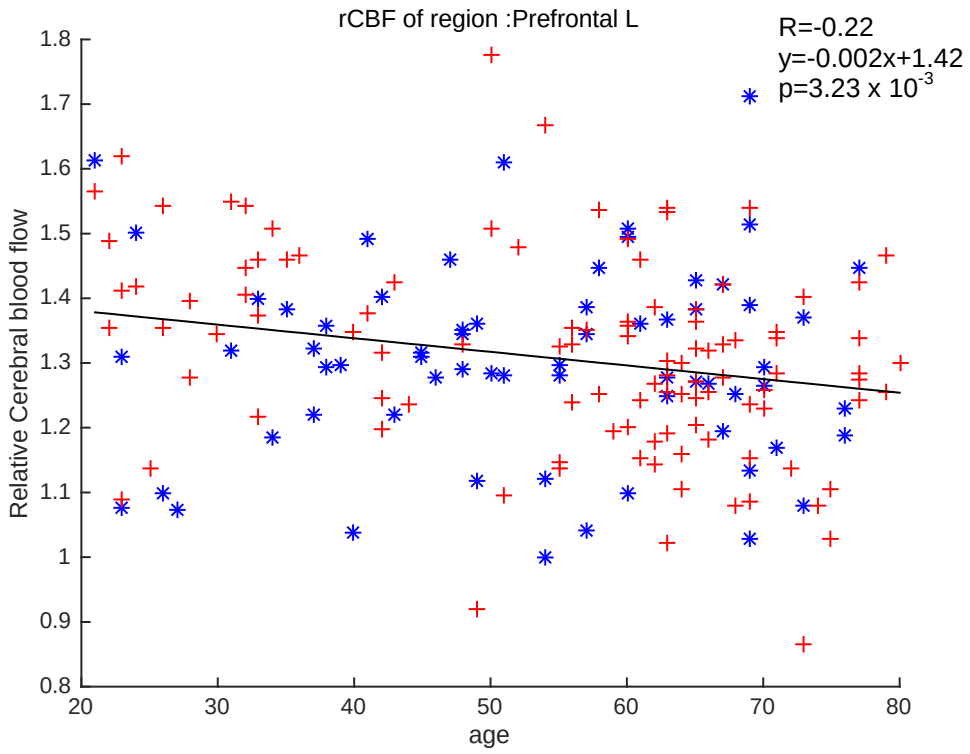

Figure 4-31 rCBF of Prefrontal Cortex Left (blue '*' represents male, red '+' represents female)

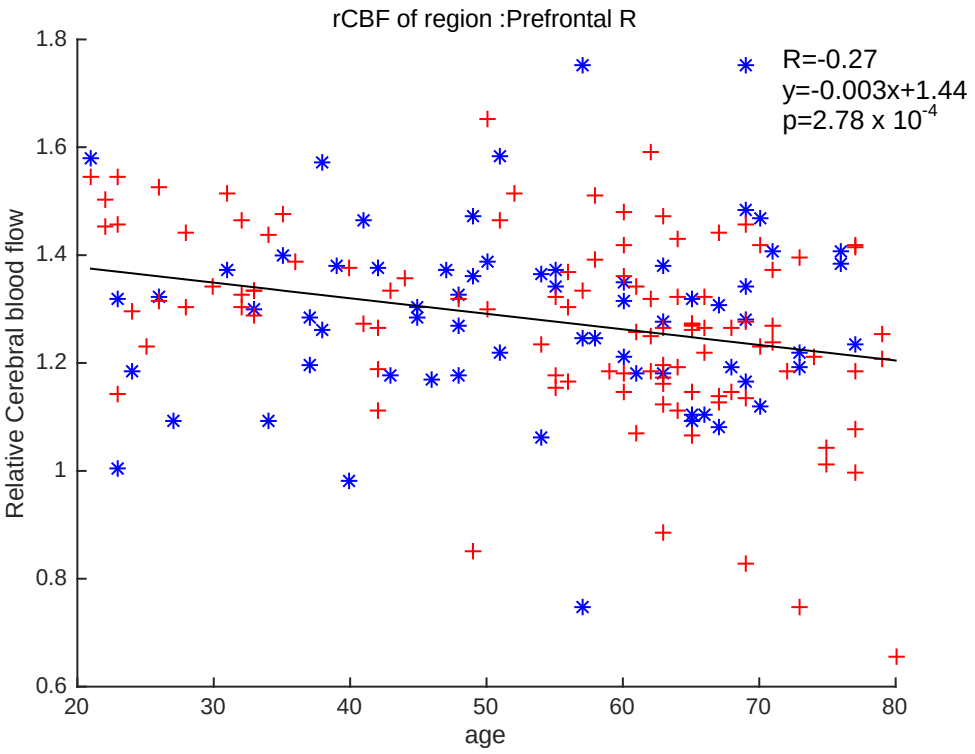

Figure 4-32 rCBF of Prefrontal Cortex Right (blue '*' represents male, red '+' represents female)

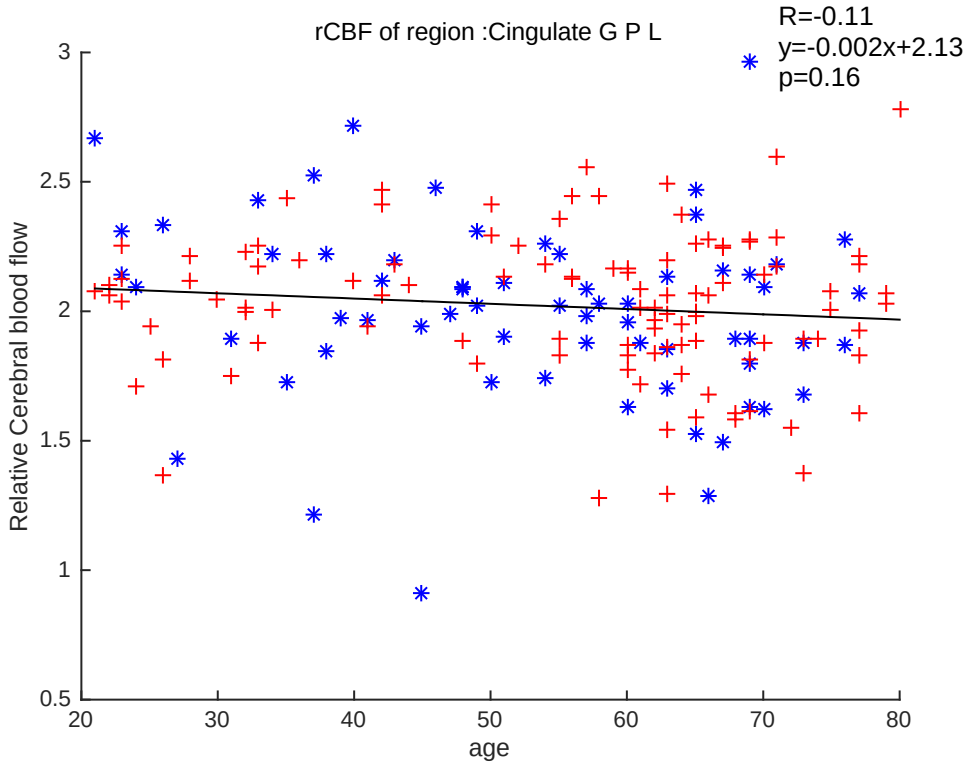

Figure 4-33 rCBF of Cingulate Cortex Posterior Left (blue '*' represents male, red '+' represents female)

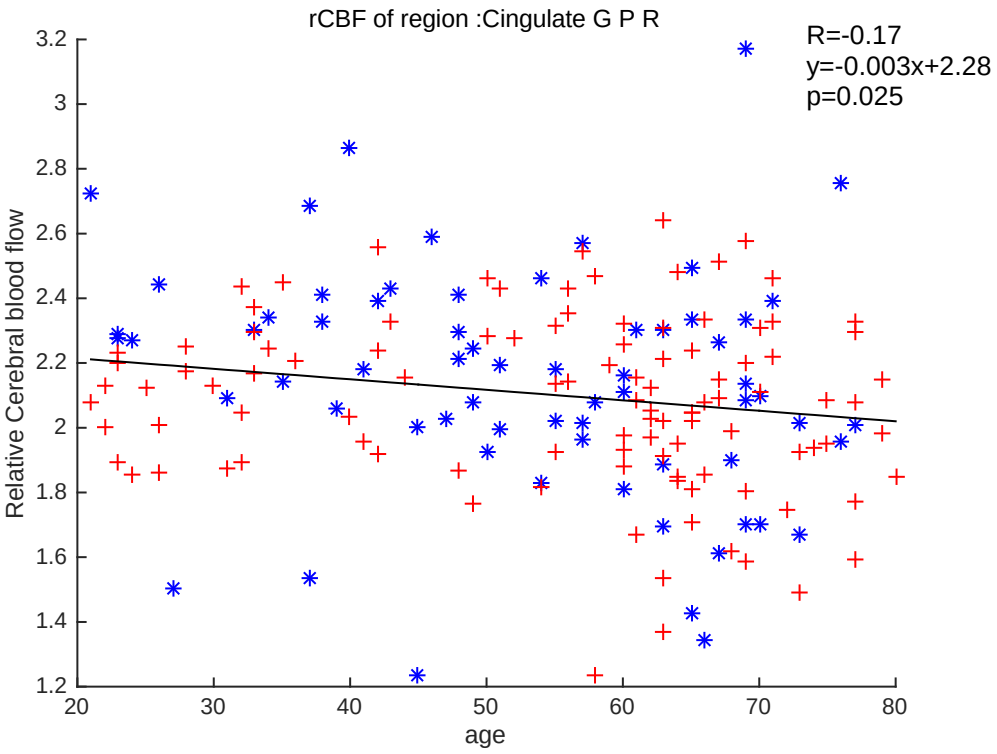

Figure 4-34 rCBF of Cingulate Cortex Posterior Right (blue '*' represents male, red '+' represents female)

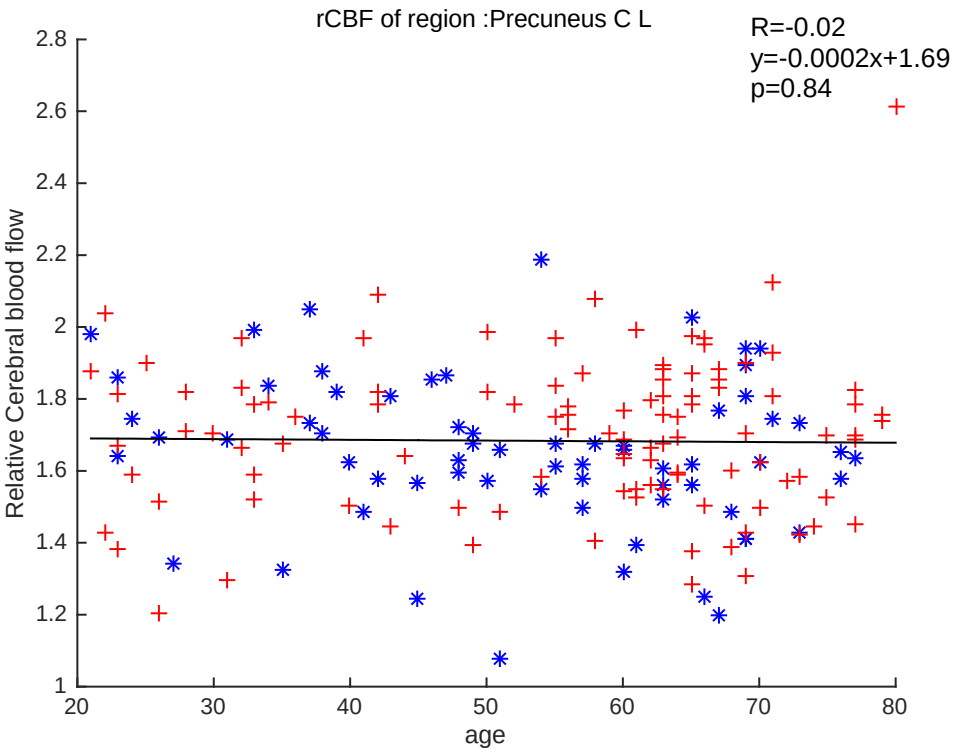

Figure 4-35 rCBF of Precuneus Cortex Left (blue '*' represents male, red '+' represents female)

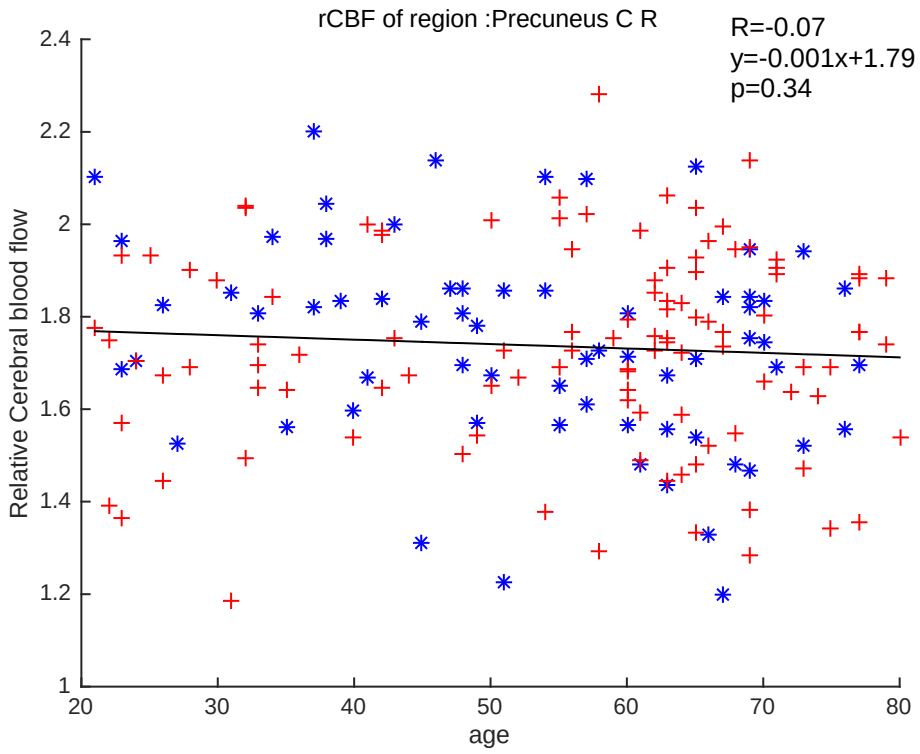

Figure 4-36 rCBF of Precuneus Cortex Right (blue '*' represents male, red '+' represents female)

According to the figure 4-4 to 4-20, CBF and rCBF decline is most significant in prefrontal cortex during aging. CBF of occipital lobe was not affected by aging too much. CBF of frontal, prefrontal, temporal lobe and hippocampus, especially right hippocampus has strong negative relationship with aging. rCBF has strong negative correlation with age in prefrontal cortex and strong positive correlation with age in white matter area, especially left hemisphere. Although not very significant, Cingulate Cortex Posterior seems to be negatively correlated with age because although the correlation coefficient is not very significant, the slope of regression line is quite significant.

Chapter 5

Discussion and Future work

5.1 Discussion

The observation that rCBF measured in white matter was positively correlated with age is because of the mathematical way of rCBF calculation. While the CBF in white matter does not change too much, the total CBF of the whole brain decreases. While the numerator does not change too much but the denominator decreases, the result seems to increase. According to other studies, CBF of white matter does not change too much according to aging [1,20]. According to one study, the change of CBF in white matter is only 3.0% per decade, but the CBF change in grey matter is 7.4% per decade [20].

The problem is that according to other studies and PET golden standard, CBF of white matter is about 20-30 ml/100g/min. Our data has the CBF of white matter as about 35 ± 7 ml/100g/min. The CBF of other areas are close to the results of other studies. So that these raise a question about if the result of white matter CBF is reliable or not. As the MR signal amplitude of the labeled blood depends on the post labeling delay, when the post labeling delay is different between brain regions, there might be some bias in CBF estimation. According to a study using pulsed ASL (FAIR), perfusion signal of white matter is significantly weaker than grey matter because the arterial transit time (ATT) of white matter is much longer than grey matter, besides, the CBF of white matter is much lower than the CBF of grey matter, so, the signal to noise ratio of CBF in white matter is lower than grey matter. The average delay of arterial transit time between grey matter and white matter is about 0.65 second, but the heterogeneity between each kind of tissue is large [37]. Because of the low resolution, there are partial volume effects that result in overestimation of white matter CBF. Although T1 image of the same subject with 1 mm cube resolution is good enough for grey matter and white matter segmentation, but the

border between grey and white matter contains a lot of voxels, and the CBF in these voxels might increase the CBF of white matter and decrease the CBF of grey matter.

Because of the relatively long and heterogeneous ATT of white matter, and the relatively low signal to noise ratio, it might not be a good idea to use ASL to get the CBF of white matter. For mild cognitive (MCI) and Alzheimer disease patients, their ATT might even longer, so that it may be difficult to get precise CBF without getting their ATT in advance and using a PLD that fits their relatively long ATT.

Of course, a 3 Tesla MR machine and Pseudo-continuous ASL increases signal to noise ratio. But according to another study also using a 3 Tesla MR machine and Pseudo-continuous ASL, in compare with ^{15}O-water PET, the reliability of CBF of white matter measured by pcASL was 0.82 in elderly subjects, but 0.931 in young subjects according to an intraclass correlation coefficient (ICC) test [1].

5.2 Limitations

There are some limitations in this study.

For ASL technology itself, there are some limitations.

First of all, the signal to noise ratio is quite low in ASL, so that it is sensitive to background noise. Secondly, Pseudo-continuous ASL is not strictly an adiabatic inversion, so that it is sensitive to magnetic field inhomogeneous, and the labeling efficiency depends on blood flow velocity, which depends on physiologic conditions [8]. Finally, low resolution of CBF map might contain some cross contamination voxels between different tissue types.

For this study, the biggest limitation was that the ASL sequence was fixed. The MRI scan was done by University of Texas Southwestern Medical Center, only post processing was done in this study. The result was affected by the ASL sequence.

First of all, without a background suppression pulse, the signal to noise ratio is not very high. As long as the ASL signal is very weak, a lot of noise might be included. This might be one reason why this study had a relatively high CBF of white matter in compare with other ASL studies.

Secondly, the M0 used in this study was the average M0 of the whole brain. There are so many different kinds of tissue with different M0 in the brain; using an averaged M0 decreased the accuracy of CBF calculation. A proton density image can be used to calculate voxel wise M0 if available.

Thirdly, the ATT between different subjects are different. A fixed PLD, which was only a bit longer than the ATT of grey matter, was used. Single PLD is robust in measuring CBF only when CBF is not sensitive to ATT. But as long as all the subjects in this study were relatively healthy, using a single PLD might be good enough.

Finally, only T1 relaxation time of arterial blood was used in the M0 and CBF calculation. In white matter, T1 relaxation time should be different from arterial blood. In another study, T1 of white matter was used in M0 calculation of each voxel from a proton density image [1].

5.3 Future Work

There are two problems quite common in ASL technique. One is that the low signal to noise ratio due to low ASL signal. As mentioned before, the difference between labeled image and control image is very small, so that it is very sensitive to noise. Pseudo-continuous ASL with large gradient and 3 Tesla MR machine do improve signal to noise ratio, but new technology is still needed to improve signal to noise ratio.

There is a balance between arterial transit time (ATT) and labeling signal strength. If the PLD is long enough to ensure that all labeled blood goes into the image plane, the signal will be too low to get a good signal to noise ratio. But if PLD is not long

enough, patients who have occlusive vascular diseases may have a low CBF because their ATT is long. Of course, ATT in different brain regions are different. How to make PLD long enough to meet the criteria of PLD > ATT without compromise the labeling signal strength is another thing, which needed to be figured out in the future.

ASL is sensitive to head motion. Even though the longer the labeling duration the better, a too long scanning time will cause more head motion. How to reduce head motion artifact needs to be study in the future.

The CBF image processing needs further study. For example, how much of smoothing is needed? Too little smoothing includes a lot of high frequency noise, but too much smoothing increases cross-contamination of CBF between different tissue types, which is not good for getting regional CBF.

The parameters and formula of CBF calculation is still in study. For example, does T2* effect need to be included in the formula? Although the TE in this study was only 14 ms, there might still be some T2* relaxation effect [22]. What T1 relaxation time should be used in calculating M0 and CBF needs further research.

References

1. Xu, G., Rowley, H. A., Wu, G., Alsop, D. C., Shankaranarayanan, A., Dowling, M., Christian, B. T., Oakes, T. R. and Johnson, S. C. (2010), Reliability and precision of pseudo-continuous arterial spin labeling perfusion MRI on 3.0 T and comparison with ^{15}O-water PET in elderly subjects at risk for Alzheimer's disease. *NMR Biomed.*, 23: 286–293. doi: 10.1002/nbm.1462
2. Huettel, S. A., Song, A. W., & McCarthy, G. (2008). *Functional magnetic resonance imaging (2nd; 2 ed.)*. Sunderland, Mass: Sinauer Associates, Publishers.
3. Suetens, P. (2009). *Fundamentals of medical imaging (2nd; 2 ed.)*. Cambridge; New York: Cambridge University Press.
4. Essig, M., Shiroishi, M. S., Nguyen, T. B., Saake, M., Provenzale, J. M., Enterline, D., . . . Law, M. (2013). Perfusion MRI: The five most frequently asked technical questions. AJR.*American Journal of Roentgenology*, 200(1), 24-34. doi:10.2214/AJR.12.9543
5. Bernstein, M., & King, K. (2004). *Handbook of MRI pulse sequences.* Amsterdam: Academic Press.
6. Alsop, D. C., Detre, J. A., Golay, X., Günther, M., Hendrikse, J., Hernandez‐Garcia, L., . . . Zaharchuk, G. (2015). Recommended implementation of arterial spin‐labeled perfusion MRI for clinical applications: A consensus of the ISMRM perfusion study group and the european consortium for ASL in dementia. *Magnetic Resonance in Medicine,* 73(1), 102-116. doi:10.1002/mrm.25197
7. Weisskoff, R. M., Chesler, D., Boxerman, J. L., & Rosen, B. R. (1993). Pitfalls in MR measurement of tissue blood flow with intravascular tracers: Which mean transit time? *Magnetic Resonance in Medicine*, 29(4), 553.

8. Aslan, S., Xu, F., Wang, P. L., Uh, J., Yezhuvath, U. S., van Osch, M., & Lu, H. (2010). Estimation of labeling efficiency in pseudocontinuous arterial spin labeling. *Magnetic Resonance in Medicine*, 63(3), 765-771. doi:10.1002/mrm.22245
9. Santrock, J. W. (2009). *A Topical Approach to Lifespan Development (5th ed.)*. Boston, Mass: McGraw-Hill Higher Education.
10. Fjell, A. M., Walhovd, K. B., Fennema-Notestine, C., McEvoy, L. K., Hagler, D. J., Holland, D., . . . Dale, A. M. (2009). One-year brain atrophy evident in healthy aging. *Journal of Neuroscience*, 29(48), 15223-15231. doi:10.1523/JNEUROSCI.3252-09.2009
11. Baal, v., G.C.M., Lerch, J. P., Boomsma, D. I., Hulshoff Pol, H. E., Collins, D. L., Brans, R. G. H., . . . Lepage, C. (2010). Brain plasticity and intellectual ability are influenced by shared genes. *Journal of Neuroscience*, 30(16), 5519-5524. doi:10.1523/JNEUROSCI.5841-09.2010
12. Chen, J. J., Rosas, H. D., & Salat, D. H. (2011). Age-associated reductions in cerebral blood flow are independent from regional atrophy. *NeuroImage*, 55(2), 468-478. doi:10.1016/j.neuroimage.2010.12.032
13. Attwell, D., & Laughlin, S. B. (2001). An energy budget for signaling in the grey matter of the brain. *Journal of Cerebral Blood Flow & Metabolism*, 21(10), 1133-1145. doi:10.1097/00004647-200110000-00001
14. Lu, H., Xu, F., Rodrigue, K. M., Kennedy, K. M., Cheng, Y., Flicker, B., . . . Park, D. C. (2011). Alterations in cerebral metabolic rate and blood supply across the adult lifespan. *Cerebral Cortex (New York, N.Y.: 1991)*, 21(6), 1426-1434. doi:10.1093/cercor/bhq22
15. Aanerud, J., Borghammer, P., Chakravarty, M. M., Vang, K., Rodell, A. B., Jónsdottir, K. Y., . . . Gjedde, A. (2012). Brain energy metabolism and blood flow differences in

healthy aging. Journal of Cerebral Blood Flow and Metabolism : Official Journal of the International Society of Cerebral Blood Flow and Metabolism, 32(7), 1177-1187.

16. Ashby, F. G. (2011). *Statistical analysis of fMRI data*. Cambridge, Mass: MIT Press.
17. Jenkinson, M., Bannister, P., Brady, M., & Smith, S. (2002). Improved optimization for the robust and accurate linear registration and motion correction of brain images. *NeuroImage*, 17(2), 825-841. doi:10.1006/nimg.2002.1132
18. Poldrack, R. A., Mumford, J. A., & Nichols, T. E. (2011). *Handbook of functional MRI data analysis*. Cambridge: Cambridge University Press.
19. Lu, H., Clingman, C., Golay, X., & van Zijl, P. C. M. (2004). Determining the longitudinal relaxation time (T1) of blood at 3.0 tesla. Magnetic Resonance in Medicine, 52(3), 679-682. doi:10.1002/mrm.20178
20. Shin, W., Horowitz, S., Ragin, A., Chen, Y., Walker, M., & Carroll, T. J. (2007). Quantitative cerebral perfusion using dynamic susceptibility contrast MRI: Evaluation of reproducibility and age‐ and gender‐dependence with fully automatic image postprocessing algorithm. *Magnetic Resonance in Medicine*, 58(6), 1232-1241. doi:10.1002/mrm.21420
21. van Gelderen, P., de Zwart, J. A., & Duyn, J. H. (2008). Pittfalls of MRI measurement of white matter perfusion based on arterial spin labeling. *Magnetic Resonance in Medicine*, 59(4), 788-795. doi:10.1002/mrm.21515
22. Buxton, R. B., Frank, L. R., Wong, E. C., Siewert, B., Warach, S., & Edelman, R. R. (1998). A general kinetic model for quantitative perfusion imaging with arterial spin labeling. *Magnetic Resonance in Medicine*, 40(3), 383.
23. Williams, D. S., Detre, J. A., Leigh, J. S., & Koretsky, A. P. (1992). Magnetic resonance imaging of perfusion using spin inversion of arterial water. *Proceedings of*

the National Academy of Sciences of the United States of America, 89(1), 212-216. doi:10.1073/pnas.89.1.212

Biographical Information

Ciwe Wang was born in Shanghai, China on Dec. 16th 1980. She completed her Bachelors in computer science from Shanghai University of Electric Power,China in June 2004. She started her career as a computer engineer in a private company in Shanghai. She had been working in Oracle database, Red Hat Linux system administrator and Cisco network engineer for years. She got the Cisco certification in 2007. In the fall of 2010, she began her undergraduate study as pre-nursing student at University of Texas at Arlington. She was accpted by the nursing program in spring 2013 after she completed all her pre-nursing courses. She quited the nursing program after she completed her first semester in the nursing program and applied for the master program of biomedical engineer in University of Texas at Arlington. In fall 2013, she began her graduate study in biomedical engineer. In order to combine her computer knowledge with medical knowledge, she took the imaging track in her graduate study. She took MRI courses and joined Dr. Rong Zhang's research group in the institute for exercise and environmental medicine. She mainly focuses in MRI image processing, especially ASL image processing during her research. She plans to do more researches in biomedical imaging field, especially in MRI image processing field.